Sequence context and ribosome collisions affect suppressor tRNA efficacy and readthrough at PTCs

Dissertation

zur Erlangung des akademischen Grades

Doctor rerum naturalium

(*Dr. rer. nat.*)

eingereicht am

Fachbereich Chemie der

Fakultät für Mathematik, Informatik und Naturwissenschaften

der Universität Hamburg

vorgelegt von

Nikhil Bharti, M. Sc.

geboren in Delhi (Indien)

Hamburg 2023

Die vorgelegte Dissertation wurde von *March 2019 until December 2022* am Institut für Biochemie und Molekularbiologie am Fachbereich Chemie der Fakultät für Mathematik, Informatik und Naturwissenschaften an der Universität Hamburg unter Anleitung von Prof. Dr. Zoya Ignatova angefertigt.

The submitted dissertation was conducted from March 2019 until December 2022 at the Institute of Biochemistry and Molecular Biology at the Department of Chemistry of the Faculty of Mathematics, Informatics, and Natural Sciences at the University of Hamburg under the supervision of Prof. Dr. Zoya Ignatova.

Date of disputation: 12th Mai, 2023

Dissertationsgutachter / *dissertation reviewers*:

1. Gutachterin / *first reviewer*: **Prof. Dr. Zoya Ignatova**, Institute of Biochemistry and Molecular Biology, Universität Hamburg

2. Gutachter / *second reviewer:* **Prof. Dr. Daniel N. Wilson**, Institute of Biochemistry andMolecular Biology, Universität Hamburg

Zusammenfassung

Nonsense-Mutationen sind die Ursache für etwa 11 % aller genetisch vererbten Krankheiten. Sie entstehen durch eine Punktmutation in der mRNA-Kodierungssequenz, dies Veränderung verursacht ein Stoppcodon, das auch als vorzeitiges Terminierungscodon (PTC) bezeichnet wird. PTCs weisen die gleiche Identität wie die natürlichen Terminationscodons UGA, UAG und UAA auf und signalisieren somit den Abbruch der mRNA-Translation. Bei der Translation von PTC-haltigen mRNAs entstehen verkürzte und oft dysfunktionale Proteine, die sogar Gain-of-Function- oder dominant-negative Effekte haben können. Therapeutische Strategien, die auf die Unterdrückung von PTCs abzielen, um die mangelhafte Proteinfunktion wiederherzustellen, werden als Nonsense-Suppressionstherapien (oder PTC-Readthrough-Therapien) bezeichnet. Sie haben das Potenzial, für viele Patienten und bei einer Vielzahl genetischer Erkrankungen, einschließlich Krebs, von therapeutischem Nutzen zu sein. Mehrere kleine Moleküle wurden auf ihre Eignung zur Korrektur von PTC-Mutationen untersucht; das am häufigsten untersuchte kleine Molekül ist das Aminoglycosid-Antibiotikum G418. Es hat in In-vitro-Studien, in Tiermodellen und sogar in ersten klinischen Versuchen vielversprechende Ergebnisse erzielt, musste aber wegen umfangreicher Fälle von Ototoxizität und Nephrotoxizität bei Patienten bei langfristiger Anwendung eingestellt werden. Ein weiteres kleines Molekül, das von der europäischen Arzneimittelbehörde zur Behandlung der Duchene-Muskeldystrophie zugelassen wurde, war Ataluren, das jedoch ebenfalls nicht zur Behandlung der PTC-Mutationen des Mukoviszidose-Transmembranregulators geeignet war.

CFTR weist über 70 PTC-Mutationen auf, von denen die häufigsten W1282X, G542X und R553X sind. Die von uns entwickelten Suppressor-tRNAs haben das Potenzial, PTC-Mutationen mit hoher Wirksamkeit zu korrigieren, die um ein Vielfaches höher ist als bei kleinen Inhibitoren. Mithilfe von Suppressor-tRNA konnten wir PTC-Mutationen in von Patienten stammenden Nasenepithelzellen und in Laborzelllinien korrigieren. Neben der Herstellung des CFTR-Proteins in voller Länge zeigen wir dass es funktionell ist, indem wir Ansätze verwenden die als Goldstandard für den Nachweis des klinischen Nutzens etabliert sind. Mithilfe von Deep-Sequencing-Ansätzen zeigen wir, dass die Suppressor-tRNA keine erkennbaren Auswirkungen auf natürliche Terminationscodons oder auf interne Codons hat. Es ist auch bekannt, dass der mRNA-Sequenzkontext eines PTC Einfluss darauf hat wie gut eine Suppression stattfinden kann. Wir zeigen hier auch, dass der Sequenzkontext eines PTC bei der Korrektur mit Suppressor-tRNA nicht derselbe ist wie bei der Verwendung von kleinen Molekülen. Wir zeigen hier auch, dass der Kontext upstream wichtiger ist als der downstream Kontext, wenn es darum geht, Suppressor-tRNA zur Korrektur von PTC-Mutationen zu verwenden.

Abstract

Nonsense mutations are an underlying cause for approximately 11% of all inherited genetic diseases. They result from a point mutation in mRNA coding sequences which introduces stop codon called also pre-mature termination codon (PTC). PTCs exhibit the same identity as natural termination codons, UGA, UAG and UAA, and thus, signal mRNA translation termination. When translated, PTC-containing mRNAs produces truncated and often dysfunctional proteins which might even have gain-of-function or dominant-negative effects. Therapeutic strategies aimed at suppressing PTCs to restore deficient protein function collectively named nonsense suppression (or PTC readthrough) therapies have the potential to provide a therapeutic benefit for many patients and in a broad range of genetic disorders, including cancer. Multiple small molecules have been screened for correcting PTC mutations; the most widely studied small molecule is an aminoglycoside antibiotic G418. It has shown promising results in in vitro studies, in animal disease models and even in primary clinical trials but had to be discontinued due to extensive cases of ototoxicity and nephrotoxicity in patients when used long term. Another small molecule which was approved by European medical agency for treating Duchene muscular dystrophy was Ataluren, but it also failed to treat Cystic Fibrosis Transmembrane Regulator PTC mutations.

CFTR has over 70 PTC mutations of which the most prevalent are W1282X, G542X and R553X. We developed engineered suppressor tRNAs show potential in correcting PTC mutations with high efficacy, with many folds higher than achieved with small inhibitors. Using suppressor tRNA we were able to correct PTC mutations in patient-derived nasal epithelial cells and in laboratory cell lines. Along with producing full-length CFTR protein, we show it is functional using approaches established as gold standards to show clinical benefit. Using deep-sequencing approaches we show that suppressor tRNA has no discernible effect on natural termination codons or at internal codons programmed to readthrough to produce a functional protein. It has also been known that mRNA sequence context of a PTC influences how strong of a suppression is needed, we here also show that sequence context of a PTC when correcting with suppressor tRNA is not the same as when using small molecules. We also show here that upstream context is more important than the downstream context, when it comes to using suppressor tRNA to correct PTC mutations.

List of abbreviations

CFTR – Cystic fibrosis Transmembrane Regulator	RNA- Ribonucleic acid
PTC – Premature termination codon	DNA- Deoxy ribonucleic acid
bp- base pair	40s,60s,18S- Svedberg unit
eRF1- eukaryotic release factor 1	AA- amino acid
RF- Release factor	PIC- pre-Initiation complex
rRNA- Ribosomal RNA	PABP- poly A binding protein
tRNA- transfer RNA	uORF- upstream open reading frame
UPF1-up frameshift protien1	EJC- exon junction complex
NMD- nonsense mediated decay.	G418- Genticin
AA- amino acids	eIF- Eukaryotic initiation factor
GTP-Guanosine triphosphate	Fluc- Firefly luciferase
GDP- Guanosine diphosphate	AC- anti codon

CONTENTS

1. Introduction

1.1 Translation in Eukaryotes

The fate of a cell is determined by precisely exerting genetic information in the form of function. A key step for transforming genetic information into function is mRNA translation, during which genetic information passed on from DNA to protein through mRNA is decoded. mRNA decoding or translation is the final and the most energy consuming step of this cascade information relay (1). This process of mRNA decoding or protein synthesis is catalyzed by molecular ribonucleoprotein machines called the ribosome (2). The eukaryotic ribosome consists of a small

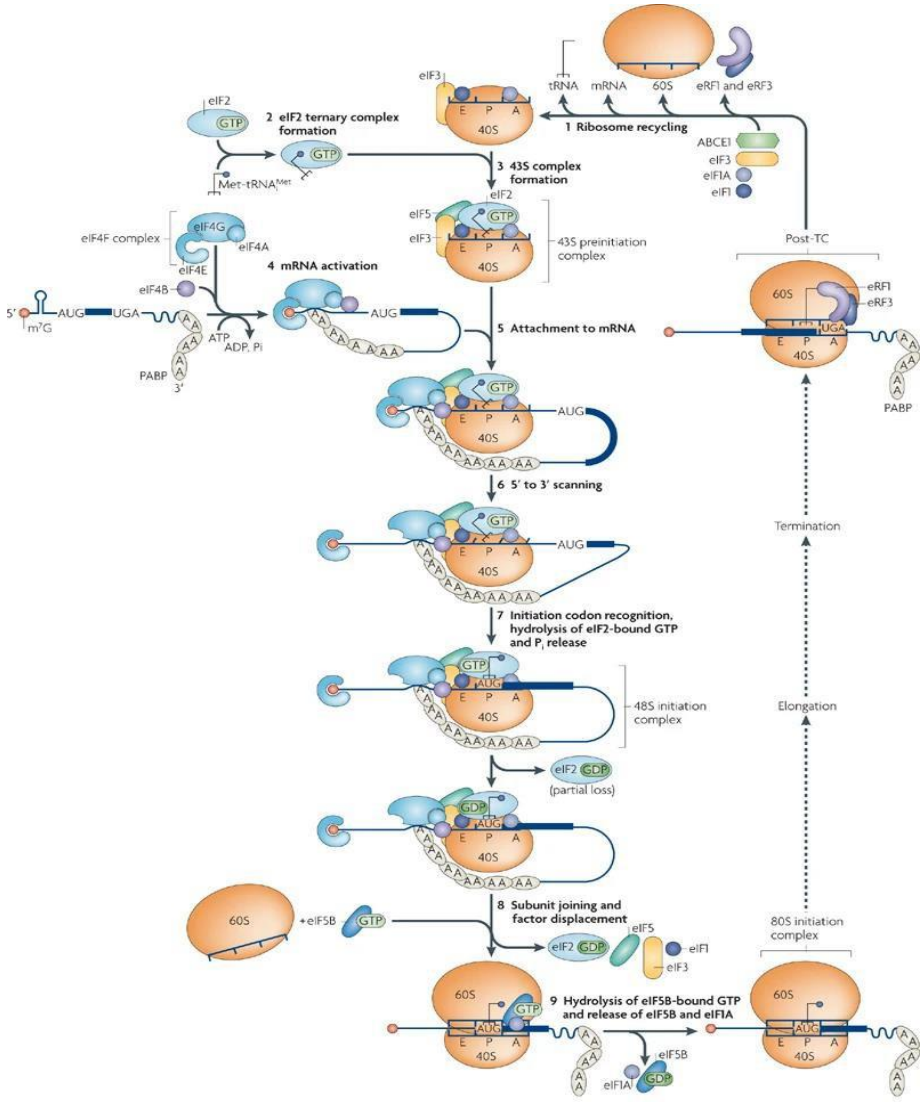

Figure 1.1: Schematic representation of translation process in eukaryotes. Translation broadly is divided in initiation, elongation and termination, which is followed by ribosome and factor recycling to continue the process again. Adopted from (6).

40S and a large 60S subunits, which together forming a 80S ribosome (2). The 40S subunit consists of the 18S ribosomal RNA (rRNA) and 33 different ribosomal proteins, on the other

hand the 60S subunit consists of 25S, 5.8S, and 5S rRNA together with 47 ribosomal proteins (3,4).Translation occurs in three distinct steps: initiation, elongation, and termination (5).

1.2 Initiation of translation

Translation initiation begins with formation of an 80S initiation complex from separate 40S and 60S subunits where Met-tRNA$_i^{Met}$ binds to the P or peptidyl site of the ribosome. The start codon of the mRNA can now pair directly with the anticodon of the Met-tRNA$_i^{Met}$ (2,5,6). Ribosomal binding at the 5′-end of the mRNA required eIF3, the eIF2/GTP/Met-tRNAi complex, ATP, and the eIF4F cap-binding complex, and is enhanced by presence of eIF4B (7). eIF4F is a heterotrimeric factor, its eIF4A (ATP-dependent RNA helicase) and eIF4E subunits along with the eIF4G550–1090 fragment of its 1,560-amino acid eIF4G subunit make the core of eIF4F with ensures sufficient for ribosomal attachment to capped mRNA ready for translation (7–9). There are groups of initiation factors that are involved in mRNA recruitment (eIF4, eIF3, PABP, and mRNA helicases) and along with those delivering Met-tRNA$_i$ to the 40S subunit (eIF2 and eIF5) in eukaryotes, are absent in bacteria (7–10). During initiation, eIF1A (IF1) and eIF1 (IF3) restructure the small ribosome unit for efficient selection of translation initiation region and the start codon (8,11) eIF1 moves away from its binding site on the small subunit, towards eIF3 (8) and once the Pre-Initation complex (PIC) closes, eIF2•GDP and eIF5 dissociate and is replaced by the 60S ribosomal subunit. This process is facilitated by the GTPase eIF5B. Upon subunit joining, which is very similar to the mechanism of subunit joining in bacteria, eIF5B hydrolyzes GTP, producing a conformational rearrangement of the 80S initiation complex, The GDP-bound form of eIF5B reduces affinity for the initiation complex, allowing it to freely dissociate after GTP hydrolysis (12,13). These intricate natures and coordinated function of various factors complete the process of initiation of mRNA translation in eukaryotes. As a whole the process is highly precise, with room for very low error. This precise selection of the start codon at the end of this process is crucial for the following step, the elongation, in which the peptide chain initiated by Met-tRNA$_i^{Met}$ is extended amino acid by amino acid reading the subsequent codons.

1.3 Elongation

Elongation at each codon entails three steps, decoding of an mRNA codon by the cognate aminoacyl-tRNA, peptide bond formation, and translocation of the tRNA–mRNA complex, which moves peptidyl-tRNA from the A site to the P site and presents a new codon in the A site (8). During elongation, the ORF is decoded in steps of three nucleotides which defines the

'codon' register or 3nt periodicity in translation. The elongation cycle starts with a peptidyl-tRNA in the P site and an empty aminoacyl and exit site. Elongation entails three steps, decoding of an mRNA codon by the cognate aminoacyl-tRNA, peptide bond formation, and translocation of the tRNA–mRNA complex, which moves peptidyl-tRNA from the A site to the P site and presents a new codon in the A site (8) In contrast to the complex factor requirements in translation initiation, elongation is assisted by a minimal set of factors. In addition to the canonical factors eEF1A (bacterial homolog EF-Tu) and eEF2 (bacterial homolog EF-G), the elongation factor eIF5A (bacterial homolog EF-P) is also conserved between eukaryotes and bacteria(6). The eukaryotic elongation factor 1 (eEF1) comprises eEF1A and eEF1B. eEF1A delivers aminoacyl-tRNAs to the A site of the ribosome as reaches empty to the subsequent codon. Factor eEF1A is a member of the GTPase superfamily which binds and hydrolyzes GTP. The dissociation of GDP from eEF1A is accelerated by a guanine nucleotide exchange factor (GEF), eEF1B, which is composed of two subunits, eEF1Ba and eEF1Bg, in yeast, or three subunits, eEF1Ba, eEF1Bg, and eEF1Bb, in mammals (8). As soon as aminoacyl-tRNA is accommodated in the A site, it forms a peptide bond with the P-site peptidyl-tRNA. The peptidyl transferase center of the large ribosomal subunit is highly conserved of rRNA elements the speculation is that the reaction mechanism is the same in prokaryotes and eukaryotes (8,14) Yeast eEF1A binds aminoacyl-tRNA in a GTP-dependent manner and promotes its binding to the mRNA-programed 80S ribosome. Yeast eEF1A·GTP binds aminoacyl-tRNA with nanomolar affinity After the ternary complex is formed, aminoacyl-tRNA delivery to the A site of the eukaryotic ribosome (8,15).

1.4. Termination of translation

The termination of protein synthesis has traditionally been referred to as the polypeptide release factor mediating release of the completed polypeptide from the ribosome. This occurs in response to the ribosome encountering a stop codon in the decoding site. Understanding this last phase of protein synthesis has been slower and less understood than compared to other events of translation, partly because it has been difficult to establish appropriate in vitro systems to study the event. Earlier prevalent perception suggested that termination is of less profound significance to the cell. It is now clear that the efficiency of reading stop signals can be very important in the regulation of certain cellular events. Translational termination can be thought of in two ways: either as a complete stop in protein synthesis mediated by the polypeptide chain release factor (RF), the general and fundamental event resulting in release of the protein product, or as a pause at these stop signals, the signals being used as a "give way" (or "yield") for more specialized purposes (16). Translational stopping involves an intimate coordination between the ribosome,

the mRNA, and the polypeptide release factors but the pause may allow a diverse array of competing events to take place, such as specific amino acid incorporation.

Translation termination takes place when the end of the coding sequence is reached by the ribosome and a stop codon (UAA, UGA, or UAG) enters the A site. Termination in eukaryotes is catalyzed by two release factors, eRF1 and eRF3, that appear to collaborate in the process (17–19) eRF1 is omnipotent, that is, it is responsible for recognition of all three stop codons and induces release of the nascent polypeptide from the P-site peptidyl-transfer RNA (tRNA), whereas eRF3 is a GTPase that enhances polypeptide release. The resulting post-Termination complex is recycled by splitting of the ribosome, which is mediated by ABCE1. This step is followed by release of deacylated tRNA and messenger RNA (mRNA) from the 40S subunit via redundant pathways involving initiation factors such as eIF2D. Recycling enables ribosomes and mRNAs to participate in multiple rounds of translation (20).

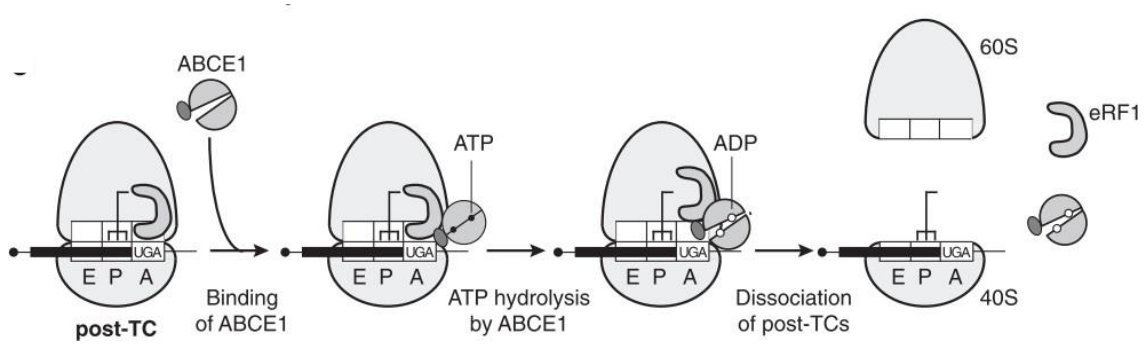

Figure 1.2: Model for ribosome recycling. ABCE1 binds to eRF1 on the post-termination complex (post-TC), and ATP hydrolysis leads splitting of t the post-termination ribosome, with releases 60S subunit, eRF1, ABCE1, and a 40S subunit which was still bound to messenger RNA (mRNA) and deacylated transfer RNA (tRNA). Adopted from (21).

1.4.1 Recognition of termination codon

Termination is mediated by eRF1 and eRF3 eRF1 has an amino-terminal domain (N) that is responsible for recognition of the stop codon in the A site a middle domain (M) containing a universally conserved apical GGQ motif that induces release of the nascent polypeptide from peptidyl-tRNA in the ribosomal P site and a carboxy-terminal domain (C) that binds to eRF3 and ABCE1, and contains a mini-domain that affects stop codon specificity (19,21,22). eRF3 consists of a non-conserved amino-terminal domain that is not required for eRF3's function in termination but binds the poly(A)-binding protein (PABP) (23,24) and the nonsense-mediated decay (NMD) factor UPF3b (25). There are two isoforms of eRF3 that are encoded by different genes and have

different amino-terminal domains; both bind eRF1 and are functional termination factors. eRF3b is predominantly expressed in brain tissue, whereas eRF3a is ubiquitously expressed eRF1 enhances binding of GTP to eRF3 by acting as a GTP dissociation inhibitor, promoting formation of a stable eRF1/eRF3•GTP complex (26,27). eRF1 is somewhat a tRNA-shaped protein if taking the liberty of looking alike comparison (28). The amino-terminal domain is responsible for codon recognition and contains a distal loop with a highly conserved NIKS motif which basically 'decodes' the stop codon via through codon:anticodon-like interactions. Chemical crosslinking experiments previously done have suggest that this loop is indeed in close proximity to the stop codon nucleotides (29). Other regions of eRF1 also appear to contribute to stop codon recognition including the YxCxxxF motif (30,31). Overall, the findings in eukaryotes suggest that stop codon recognition is more complex that was understood previously and also compared to the counterpart in prokaryotic systems.

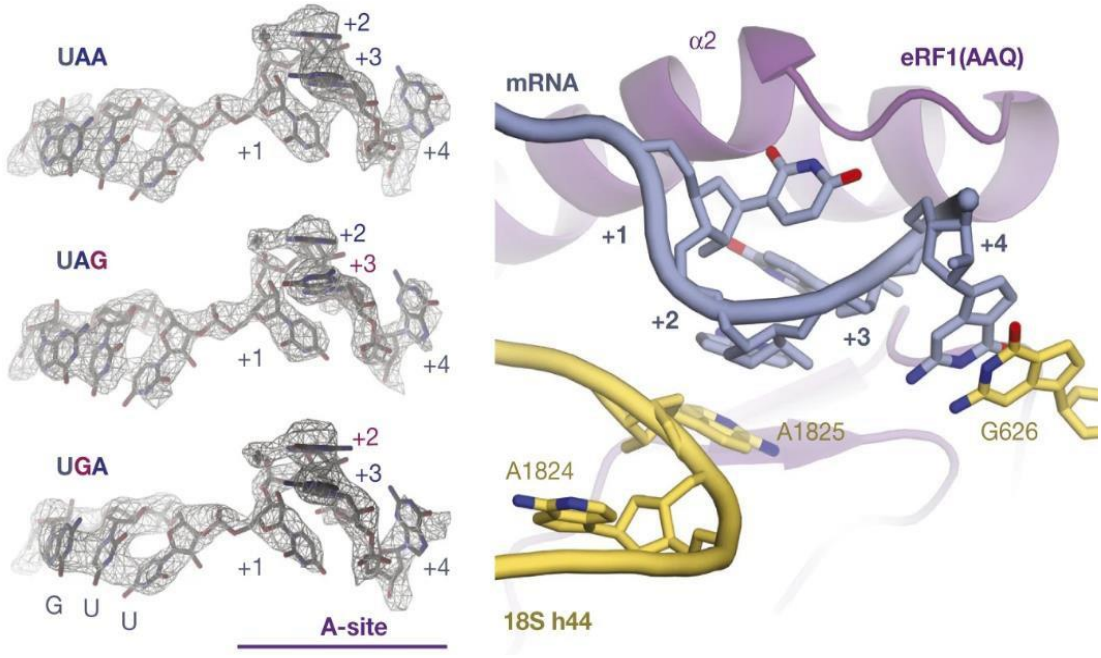

Figure 1.3: Stop codon configuration in the eukaryotic decoding center. From left to right: First., Electron microscopy map densities (at 0.12–0.17 eA˚23) of the mRNA in each termination complex reveal the same compacted conformation, eRF1(AAQ) (purple) recognizes four mRNA bases (11to 14, slate) in the A-site. Second., Bases +2 and +3 stack on A1825, and base +4 on G626 of 18S rRNA. Showing interaction of +4th base right after the stop codon interactions with the ribosome during translation termination. Adopted from (32).

1.4.2 Termination is more than terminating at defined 3-nucleotide stop codon

The canonical genetic code has three stop codons (UAA, UAG, and UGA), but the efficiency of termination is facilitated by other nucleotides flanking the stoo codon. For example, a purine residue in the +4 position and by a +5 purine when +4 residue is a pyrimidine enhance termination (33). In eRF1-bound ribosomal complexes, the N domain reaches into the A site, forming a pocket that accommodates the stop codon and the +4 nucleotide in a compacted conformation this compacted state and eRF1's interactions with the stop codon are likely maintained throughout the termination process until eRF1 is dissociated from the ribosome proceeding which splitting and further recycling occurs (34). Stabilization of the compacted state requires a +1U, which is a determinant of stop codon recognition, as are the stacking interactions of the +2, +4, and +5 nucleotides with A_{1825}, G_{626}, and C_{1698} of 18S rRNA, respectively, as well as the stop codon's multiple interactions with eRF1 (28). The stabilizing interaction of the +1 uridine with N_{61} and K_{63} of the TASNIKS motif would not be possible for cytidine at this position steric hindrance also does not allow a purine at this position. Interactions of the YxCxxxF motif and E_{55} with +2 and +3 nucleotides happens only when purines are there, it is also shown that T_{32} of the GTS motif can hydrogen bond with the +3 nucleotide of UAG but not UGA or UGG codons (32,35) With the GTS motif being flexible and highly accurate, and the mutual repulsion of G residues at +2 and +3 positions, ensures discrimination against UGG codons by eRF1. These studies are consistent with site-directed cross-linking analysis of stop codon/eRF1 interactions (16,29,31,36,37). Stop codon recognition is much more complex than was thought earlier, more research was discovered in the process of correcting PTC mutations. Factors that are responsible for recognition of PTC as a true stop codon is discussed in length in the later section 3 of sequence context as a determinant of stop codon readthrough.

2. Fidelity of translation termination

Many studies have established the roles of eukaryotic translation termination factors eRF1 and eRF3 in directly interacting with the vacant ribosome A site, i.e. when there is no aminoacylated tRNA, and finding the stop codon (19,38,39). Recent studies that directly monitor kinetics of the individual termination steps reveal that a pre-bound complex of eRF1, eRF3 and GTP (ternary complex) rapidly finds the empty A site at a stop codon (19,39). The eRF1 binding is facilitated by its conformational changes that are unlocked by eRF3 and followed by a relatively slow dissociation compared to binding in a concentration independent manner (40). This has been a consistently described in other studies as well which show that free eRF1 is unable to bind to the

empty A site of the ribosome (28,34) and also not even in concentration dependence manner (32,36). After establishing that eRF1 works as a component of tertiary complex with eRF3 and GTP, RF3 release is responsible for positioning the eRF1 into the active conformation in the empty A-site of the ribosome, which is possible after eRF3 hydrolysis GTP promoting its release (34,40). The downstream processes of ribosome splitting, and peptide release can now take place right after eRF3 is released and leaving confirmatively active form of eRF1 in the A-site, thereby releasing the peptidyl tRNA bond by rapidly cleaving it. This in turn triggers ribosomal intersubunit rotation, a movement of the deacylated P-site tRNA to a P/E hybrid state, and ejection of both eRF1 and liberating the peptide. The interdependence of these events cannot be understated, also the sequential manner in which these events occur are very much responsible for maintaining the fidelity of eukaryotic ribosomal termination. The interdependence was solidified when showing that eRF1 releases slowly in presence of drugs such as G418 and puromycin which basically binds to ribosome and stops the intersubunit rotation (41). When directly tracking the peptidyl-tRNA bond hydrolysis, it was found that these small molecules basically hinder the discrete steps which follow ‘termination’ of eukaryotic ribosome, allowing for readthrough at the stop codon (40). Eukaryotic termination is approximately 4s long, that is much faster than initiation (approximately 20-30s), but at the same time is relatively slower compared to elongation 0.05-1.4 codons/s (40). The total eukaryotic termination time is a culmination of discrete steps from eRF1-eRF3-GTP binding through subsequent steps, as explained above, to splitting of the ribosomal subunits. The binding of eRF1 is not the rate limiting step as longer ribosome protected fragments (RPF) are in much higher number compared to shorter RPF (21 nucleotide reporting on rotated ribosomes with an empty A site RPF) (16,42,43). Single molecule studies have also shown that indeed that eRF1 binding is much shorter compared to the subsequent termination steps (40). Where fidelity of eukaryotic translation elongation is governed by kinetic of eEF1A (eukaryotic elongation factor-1)-tRNA-GTP (ternary complex), eukaryotic translation termination also takes similar pattern using a ternary complex using eRF1-eRF3-GTP for detecting the stop codon and bringing translation to halt. eRF3 as a factor increases specificity up to 2600-fold (40), which maintains specificity of termination. Inclusion of premature termination codon in mRNA poses big problems as the efficient termination machinery can detect these PTCs and lead to release of incomplete polypeptide change. Other secondary quality control mechanisms such as Nonsense Mediated Decay (NMD) (44) can also be activated on these mRNA which subsequently lead to degradation of the ‘faulty mRNA’, which makes correcting the PTC even more difficult.

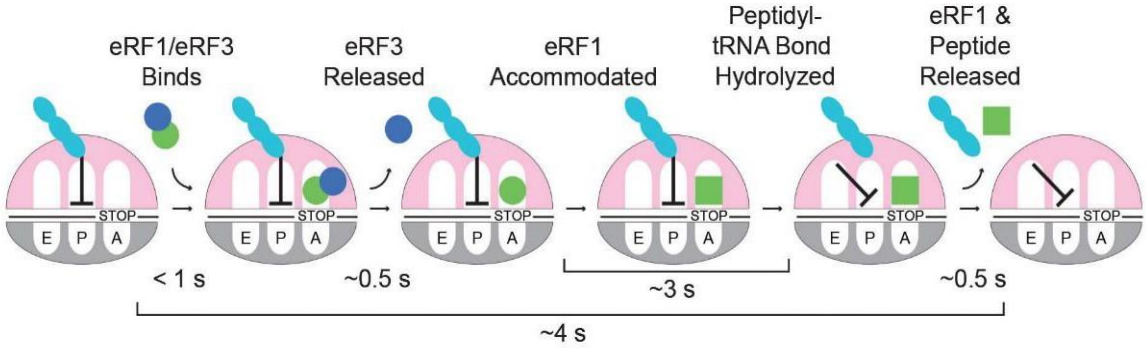

Figure 1.4: Order and timings of eukaryotic translation termination. Schematic showing how total time for a termination even is 4s which is much slower than elongation, but eRF1-eRF3-GTP complex binds to the empty A-site with an order of less than 1s, which is very similar to translation elongation time. The fidelity of translation termination is determined by these events which are highly orchestrated and conserved to efficiently recognize stop codon. Adapted from (40).

2.1 Non-sense mutations

Non-sense mutation or occurrence of pre-mature termination codons (PTC) in the coding region of mRNA are formed due to mutations. These mutations are a reason for multiple pathologies all around the world, phenotypes of these mutations have been considered to be among the most harmful ones for humans (45). Occurrence of one lead to premature protein translation termination and results in a non-functional polypeptide release (45). Non-sense mutations or loss of function mutations include insertions and deletions that alter the reading frame of a gene by altering its length (46). This alteration happens when normal amino acid coding codon changes to a stop codon, for humans which are UGA, UAG and UAA, signaling for end of protein translation, they do not encode for any amino acid hence a ribosome encountering these stop codons halts with an empty A-site. PTCs can affect phenotype of the organism in various ways, they even account for 20% of all disease associated mutations (47). Basically, frequency of the genes where PTC are prevalent dictates deleterious nature of the mutation. Many different diseases are caused by these PTCs and present as clinical phenotypes for instance; Non-sense mutation in GDF2 gene coding the bone l was found to be the cause of systemic lupus erythematosus (48), a nonsense mutation in the PRNP gene was associated with clinical Alzheimer's disease (49), Furthermore, a nonsense mutation in the TITF1 gene was observed in a family with benign hereditary chorea etc (50). One of the genes that has over 70 PTC mutations in patients with varying phenotypic effects is cystic fibrosis transmembrane regulator or CFTR. (https://cftr2.org/) CFTR is an autosomal recessive disease and the disease model for this thesis.

2.1.1 Cystic Fibrosis Transmembrane Regulator (CFTR)

As described above CFTR is main disease model of this thesis due to varying PTC present in its mRNA, with high number of PTC and varying phenotypic effects in the population it poses difficulty in finding its cure. The CFTR protein is a member of the ATP-binding cassette class C (ABC-C) family (51,52). Consistent with other proteins in this class, it contains two membrane-spanning domains (MSD1 and MSD2) and two nucleotide-binding domains (NBD1 and NBD2) that require ATP binding for channel gating. In addition, (53,54) CFTR exhibits a unique feature not found in other ABC family members, an intracellular regulatory domain (R domain) that normally requires phosphorylation for channel opening. Improper CFTR channel function leads to dysfunction of epithelial tissues in the lung, gastrointestinal tract, pancreas, and reproductive system. There have been in general more than 2000 variants of CFTR gene mutations and most of them are disease causing (55). Due to multiple mutations, they have been characterized in six different classes, out of which PTC mutations or no protein mutations are class1 mutations

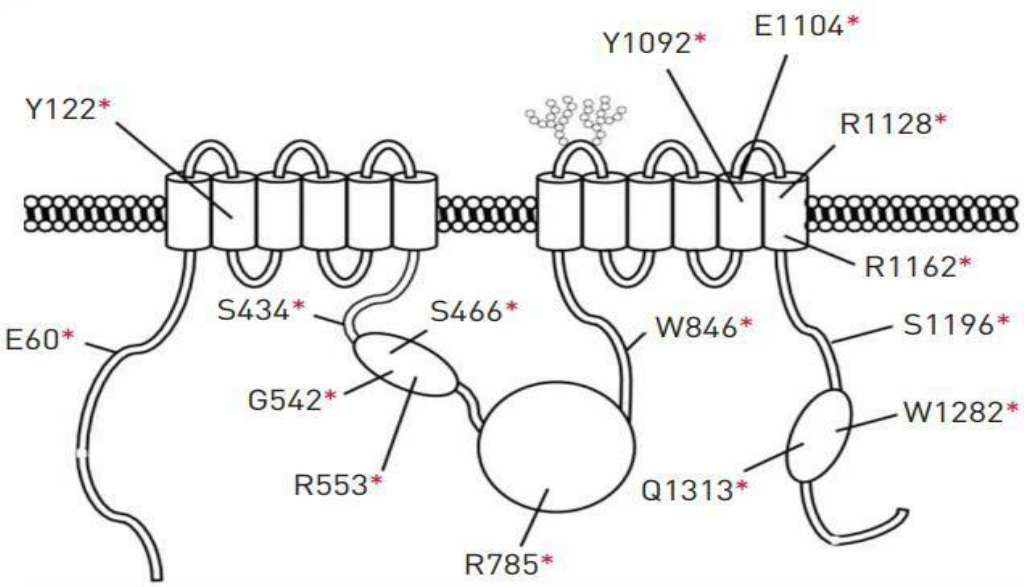

. **Figure 1.5: CFTR protein diagram with various PTC mutations**: A diagram of CFTR protein showing various major PTC mutations spread across the length. Adopted from (56).

Several therapeutics have been researched to correct non-sense mutations for CFTR and in general. Some of these small molecules or 'CFTR modulators' are known to restore expression in studies in-vitro. Class 1 mutations in CFTR affect more than 11% of CFTR affected patients (57). Some of the mutations that are high in prevalence and resistant to most of therapeutics researched are: R553X, G542X and W1282x. (www.cff.org) Along with the presence of these mutation in the coding sequence of the gene causing sudden stop in translation and production of truncated protein, these mRNA are vulnerable to a different quality control mechanism of the

cell called nonsense mediated decay or NMD. mRNA that are vulnerable to NMD are subject to degradation by various machinery in the cell (57). Lack of available correctable mRNA is one of the major issues that makes PTC mutation hard to cure.

2.2. mRNA quality control mechanisms

As mentioned in the previous section that mRNA that harbor a PTC are subjected to one of the quality control mechanisms of the cell called NMD. This quality control mechanism ensures that affected mRNA does not translate into non-functional polypeptide chains that could be toxic to the cell. In turn for this quality control, NMD ensures that the affected mRNA is no longer available to translate in a non-functional polypeptide. This reduced concentration of mRNA in the cell poses a difficulty in finding therapeutics for PTC mutations. NMD mechanism have been studied for a while, but various research has still not come to a common mechanism that elucidates clearly how NMD occurs in cell, many reports have also suggested that there may not be a 'one fits all' mechanism of NMD in cell and there can be various mechanisms in cell that regulate NMD and its factors. Up to 10% of all mRNAs in humans are subjected to this quality control mechanism (58–61). The exact mechanism via which NMD and its degradation machinery partners select their substrate is not clearly understood. At the same time several mRNA features that have been found to be a common feature in the event of NMD trigger have been associated with NMD substrate selection (62). mRNA features like: length of 3' UTR region which spatially separated the translation termination codon form the poly -A binding protein or PABP,(63,64) upstream open reading frames or uORFs, introns containing 3'UTRs, placement of exon-junction complex or EJC and the classical pre-mature codon. Most of these features have also independently shown to trigger NMD in-vitro, which also coincides with the fact that NMD can also occur independent of a PTC on an mRNA (65). Major factors that are involved in NMD machinery are UPF1, UPF2 and UPF3. In humans UPF1 is a phosphoprotein which can both phosphorylate and dephosphorylate its own cycle. UPF1s helicase activity has been found to be extremely crucial for NMD (58,66,67). NMD factor UPF1 is he major trigger for NMD response and in case of PTC is generally followed by eRF1 binding at the empty A-site of the ribosome (65).

Current models of NMD in case for a PTC suggests that NMD can ensue independently of a stable ribosome stalling and the difference of kinetics of a natural termination codon stopping the translation versus an aberrant termination at a PTC is majorly a determining factor for NMD to ensue (68). The idea suggests that NMD ensues when the ribosome at the termination codon fails to release properly from the mRNA due to mis-interactions with the trans-acting factors of

termination such as PABP and eRF3 (69). According to another the proposed model, UPF1 and the SMG1 complex subsequently form a complex with UPF2 that in a classical NMD substrate is associated with an exon-junction positioned downstream from the PTC on the mRNA. This leads to the formation of the decay-inducing (DECID) complex (58,70). In mammals, the presence of an EJC >30 nucleotides downstream from the TC functions as an important NMD enhancing factor. EJC is a multimeric protein complex deposited by splicing machinery approximately 30nt upstream of the PTC (58,71). Current literature suggests two models of NMD one which is 'EJC-dependent model' where Initially, the presence of EJCs downstream from TCs is understood to be an essential signal to identify the TC as premature and elicit NMD (72,73). Since NMD is triggered upon aberrant translation termination, which can only occur after at least one ribosome has passed the entire coding sequence and thereby removing the EJCs, NMD-targeted mRNAs without introns downstream from the TC are most likely devoid of any bound EJCs, and we therefore refer to this NMD pathway as "EJC-independent model" (74,75). Even though multiple studies have tried to fully understand mechanisms in NMD to be able to correct PTC by restricting NMD in cells, this approach have not been appreciated well as NMD is now understood to be a network of several interconnected pathways and there are no distinct routes that are understood to activate this, this makes it difficult to bypass the effects of NMD inhibition in the cell as it is essential for cells to effectively reduce targeted mRNA. NMD suppression could always pose side effects which are not even fully understood as of now. Having said that there is need to fully understand how one can induce ribosome readthrough on PTCs, but to fully understand we must understand all the factors such as NMD that have direct relationship in curing PTC mutations. Eukaryotic mRNA translation has evolved with various mechanisms to ensure that protein synthesis is highly accurate, there are several arms to quality control on of which as explained earlier is NMD. All the mechanisms are focused on ensuring correct polypeptide is released at the end of mRNA translation, in these processes termination in not occur with 100% accuracy. Ribosome A-site encountering UGA, UAG or UAA stop codons on mRNA leads to no call for a tRNA that could deliver an amino acid at these positions hence 'stop codon' but as explained in earlier sections eRF1 is the primary molecule that binds to empty-A site of the ribosome but specific interactions within the ribosome decoding center (77). eRF1 is sort of a tRNA like molecule and occupies the A-site very well with specific interactions leading to followed steps of termination (78). Termination is very much unlike elongation in eukaryotes due to lack of 'proofread' taking liberty here, proofreading during elongation ensure non-binding of a non-cognate or near cognate tRNA binding. This proofreading is done by discreet steps of initial selection and a proofread step, both of these steps are separated by hydrolysis of GTP and rely on difference in stability of codon-anticodon matches (79). Therefore, the recognition of the cognate aa-tRNA causes a local conformational change in the decoding site eliciting a transition

from an open to a closed form of the small ribosomal subunit ensuring the subsequent hydrolysis (80). This discrimination is absent at stop codon, eRF1 has competition with other aminoacyl tRNA for stop codon and the affinity is also very high, which drives essentially termination of translation and polypeptide release. In most cases the release factors outcompete the aa-tRNAs but in rare cases a near cognate tRNA can bind to the A-site of the ribosome resuming polypeptide chain synthesis and elongating it to the next in -frame stop codon, called as ribosome readthrough (78). This lack of efficient proofreading at translation termination along with this short period between ribosome reaching stop codon with empty A-site and release factor binding provides opportunity for developing readthrough agents.

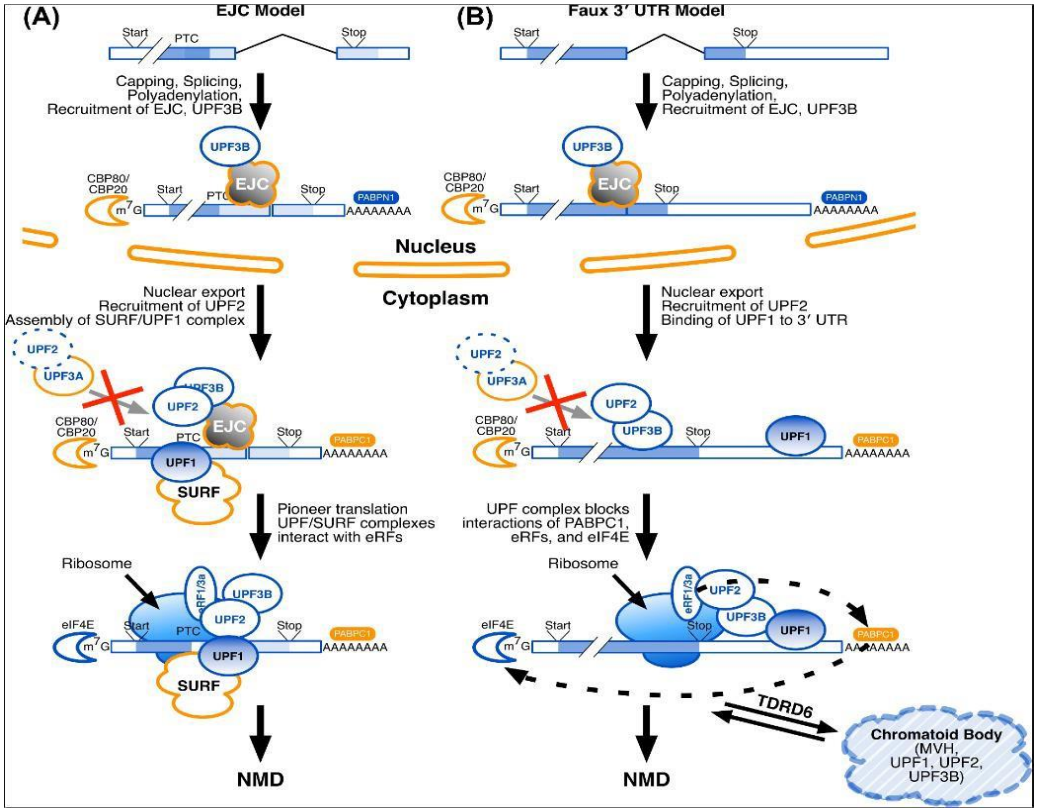

Figure 1.6: Different models of nonsense-mediated decay (NMD. (Left) In the Exon Junction Complex (EJC) model, after splicing, EJC proteins bind at the junctions of the last and penultimate exons, to be joined by UPF2, the SMG1C/UPF1/eRF1/eRF3 (SURF) complex proteins, and UPF1. A pioneer round of translation ensues, and translational release factors (eRF1 and eRF3a) allow the ribosome to recognize the stop codon. If the stop codon is premature, that mRNA is targeted for degradation. (Right) The Faux 3′ UTR model is similar to the EJC model in its nuclear marking steps. In the cytoplasm, UPF2 binds to UPF3B. UPF1 binds to multiple RNA sites within the 3′ UTR. In a way that is not yet understood, multiple copies of UPF1 might bind to a long 3′ UTR will interfere with an interaction between the release factors (eRF1, eRF3a) and PABP. Adopted from (76).

3.0. Therapies for PTCs: Many readthrough techniques/methods that have been developed are designed to take advantage of termination window.

One of the most studied drugs is an aminoglycoside antibiotic G418 or geneticin (41). One of the earliest studies with G418 was shown to suppress nonsense mutations in CFTR gene and was able to produce a functional full-length protein (41,81,82). The model has been applied to many other diseases with PTC and have been shown to produce positive results, via multiple reporter system, disease models and even clinical trials (83). G418 basically binds to the decoding center of the ribosome and allows lower discrimination of near cognate tRNA taking advantage of prolonged termination step, thereby inducing readthrough (84,85). With all the success in in-vitro experiment to clinical trials, it failed as a therapy for the patients due to its toxicity with long-term use in patients which developed persistent and serious ototoxicity and nephrotoxicity (86,87). Later a non-aminoglycoside approach was adopted of which one of the examples was PTC124 or Ataluren, which had similar success and is even approved by European Medical Agency for Duchenne muscular dystrophy with non-sense mutations (88), but at the same time ataluren was unable to show any clinical benefit to CFTR patients and was then discontinued for CFTR use (89). Ataluren is a prime example why using small molecules have innate higher non-specificity and greater chances of inducing side effects in patients along with the fact that a small molecule does not find therapeutic use for all diseases. With this being a major problem for finding therapeutics for PTC mutations, many other solutions came into play. One of which is CRISPR/Cas9-mediated genome editing (90), which can provide the perfect one-time solution for all the PTC diseases but ethical issues and their potential off-target effects are one of the biggest hurdles for it to become a potential therapy anytime soon (91–93). With the lack of any precise and a bit more personalized therapy, suppressor tRNA showed potential and was proposed as gene therapy. Suppressor tRNA is a derivative of natural tRNA with an altered anticodon to be able to base pair with stop codons UGA, UAG and UAA. tRNA based therapy even though discovered decades ago has only shown potential in recent years, due to advancements in delivery techniques for tRNA has allowed to study their efficiency in higher organisms (94–96), along with the possibility of using natural tRNA with multiple rounds of nucleotide mutagenesis and tRNA segments combinatorial techniques (97). These advancements have made it possible to increase the efficiency of suppressor tRNA readthrough many folds higher and with a possible correct insertion of amino acid at the PTC site thereby delivering a fully functional protein.

3.1 Determinants of ribosome readthrough

Even with the possible variance in translation termination, the readthrough of natural stop codons is generally a rare event. Signals for eukaryotic termination signals are highly conserved and evolved to promote efficient translation stop. There are sometimes tandem stop codons just in case there is readthrough on the primary stop codon also nonstop decay surveillance mechanism recognizes and degrades the transcripts where ribosomes are bound to poly-A tails (98). This prevents any accumulation of short peptide formed. In general frequency by which readthrough that happens at natural stop codon is 0.001%-0.1% which is approximately 10-fold lower to PTCs which are 0.01%-0.1%, which is most (99,100) likely due to termination factors and cis-acting elements that are necessary for termination are mostly bound to 3'UTR region and poly-A tail and are closer to the natural termination codon compared to PTCs (101). One of the factors which has been discussed about before is PABP, which is known to promote termination by interacting with eRF3 (102). Distance of PTC to PABP would slow down the termination at PTC giving enough time for near-cognate tRNA to bind. As we have understood earlier that most therapies take advantage of this time. This becomes an opportunity to correct PTC mutations with different possible therapies. Even with advancements of potential therapies over the years, there are many factors on which the outcome of readthrough is dependent, of which the most important factors are discussed in a bit detail below.

3.2 Inserted amino acid at the PTC for correction.

Correcting PTC with different therapies needs correct insertion of amino acid at the site of PTC. This is one of the factors which has been overlooked and underappreciated in the pursuit of finding a treatment. Extensive studies in expression systems including humans have shown that a defined subset of aa-tRNAs are actually used by ribosome machinery during readthrough. UAA and UAG stop codons are suppressed by either glutamine, tyrosine or lysine, while UGA can be suppressed by tryptophan, arginine and cysteine (103,104). The re-insertion in case of near cognate tRNA suppressing PTC happens by mispairing at position 1 or 3 of the PTC codon. UAG PTC has earlier shown preference for mismatching at positon-1 whereas, UGA shows at position 3 and UAA at both positions (104). Moreover, the identification of the amino acids reinserted during readthrough suggested that, at the third codon position, the A-C mispairing is favored over A-G and G-G, whereas in the first position the U-G mispairing is predominant, likely due to its geometrical mimicry of a standard base pairing (105,106). With amino-acid reinsertion being one of the major determining factors for successful protein function correction, it represents as a crucial factor when designing readthrough therapies. On the other hand, suppressor tRNA is easily able to resolve this problem. Since the suppressor tRNA is designed from the

original/natural tRNA of the amino acid which became PTC, it can actually carry the right amino acid to be delivered at the PTC.

3.3 Amount of correctable transcript

The amount of correctable transcript can be co-related directly to level of NMD that can take place for the particular mutation and disease. As explained earlier there is no fixed mechanism known by which NMD occurs but has many possible cis-acting factors that makes the mRNA susceptible to NMD machinery. With presence of NMD, it can become really difficult to correct PTC, which is why there are many small molecules that have shown to aid as an adjuvant to already present therapies to correct PTC to a greater level (107). One of the recent studies have even shown NMD14 or SMG1i to achieve better readthrough in CFTR intestinal non-sense mutations when delivered along with other readthrough agents (108). Use of NMD inhibitors could potentially also affect natural defense mechanisms in the cell causing unwanted NMD suppression which is crucial for cell survival, this should be kept in mind when one designs therapies with NMD inhibitors as adjuvants (109). One of the other mechanisms by which correctable transcript is no longer available is due to aberrant splicing which can result in removal of the complete exon where PTC is located and in this case any therapy targeting suppression of PTC would be rendered ineffective.

3.4 Sequence context of a PTC

PTC sequence context is the location in which PTC is inserted, the sequences around the PTC and modifications on or around the PTC makes up the sequence context of a PTC. Sequence context have been studied in light of only small molecules like aminoglycosides such as G418, their mechanism of action being inducing excess delay in translation termination process and reducing discrimination between termination factors and near cognate tRNA (33). All three stop codons at natural termination site have been shown to be decoded with different accuracy and is now a widely established, with order of their termination capability UGA>UAG>UAA (35,110). A number of studies that have focused on understanding stop codon readthrough and its sequence context have statistically highlighted that nucleotide following the stop codon at +4 position, where +1 is the first nucleotide of stop codon has a huge influence on the PTC readthrough when using small molecules (32,111–113). As has been earlier shown as discussed that during termination at a natural termination codon, the +4 position also interacts in the vicinity of the empty ribosomal A-site, hence showing that the termination signal is a tetranucleotide sequence. Some structural studies have also shown the same and also have shown 6-fold increase in

readthrough efficiency due to changes at +4 position (114). The structural studies revealed that +4 site is stacked against G626 of 18S rRNA and also that G626 is less stable when stacked against pyrimidines compared to purines (32). This indicated that at +4 position if cytosine or uracil are present the termination is weak or read through favorable. Studies have also shown that UGAC and UGAU are the most favorable for readthrough at stop codon. The order of favorable readthrough was also shown to be UGAC>UGAU>UGAC>UAGU> UAGN>UAAC>UAAU>UAAN(115). Where UAAA is one of the most difficult to readthrough posing to be the most accurate terminating sequence. Besides these sequence various other studies have also seen statistical correlation of nucleotides upstream and downstream from -3 to +9 of PTC, upstream -2 and -1 position have also been shown to significantly affect levels of readthrough positively when both those positions had adenines (116,117). The structural basis for these effects is unclear, although the P site codon (including positions -2 and -1) appears to directly contact the top of helix 44 of 18S rRNA, and the +4 and +5 nucleotides to stack with G626 and C1698 bases of 18S rRNA, respectively (116). This highlights the presence of a complex network of interactions between ribosome and the sequence surrounding the PTC, which has been only shown when readthrough was induced by small molecules. With new therapies been developed such as use of nonsense suppressor tRNA, one must revisit sequence context and try to understand if sequence context holds any value when correcting PTC with suppressor tRNA. It could also be that the idea of sequence context may be more intricate when it comes to suppressor tRNA induced readthrough. Understanding readthrough sequence context provides value in categorizing PTC mutations in groups of their easiness to be corrected and see if variability occurs across diseases or not. Core understanding of sequence context will also provide information on more susceptible PTC mutations for which finding therapies can be hastened.

4.0 Aim of thesis

Suppressor tRNAs exist in some species to suppress some stop codons. The idea of using them to suppress PTC mutations in diseases was appealing, yet their use remained limited for many decades. New generation of engineered non-sense suppressor tRNA with specific nucleotides altered in natural tRNA along with replacing the anticodon to read UGA, UAG or UAA PTCs renders them efficient PTC suppressors by increasing their efficiency through improving their interactions with translation factors. This approach leads to new generation non-sense suppressor tRNAs with a high potential to become a safe and effective gene therapy to correct various pathologies associated with PTC mutations. Understanding how sequence context affects PTC readthrough is central to our understanding and application of readthrough agents in various pathologies. So far, this has been studied with small molecules such as aminoglycosides. There is a lack of understanding of the role and effect of sequence context in PTC readthrough when using suppressor tRNA. Also, with more interacting partners of suppressor tRNA, the earlier understanding of PTC context cannot be used as a template. The aim of the thesis was (i) to determine readthrough efficiency of suppressor tRNAs in systems that report on clinical benefit and (ii) with selected highly efficient tRNA suppressors to determine its efficacy in different sequence context. By examining long and short PTC contexts, we, we shed light on the variability in suppressing PTCs with different context, Therefore, this though map of PTC mutations correctability provides a framework to build suppressor tRNA toolbox in to treat various PTC mutations in different disease genes.

5.0 Results

The results of my thesis are subdivided in two major chapters **(Chapter 5.1 and Chapter 5.2).** Methods section represents a separate chapter following both chapters.

5.1 Repurposed tRNA suppresses nonsense mutations in CFTR patient derived cells.

In this chapter I introduce a strategy to repurpose sense-codon decoding tRNAs into efficient PTC suppressors. The suppressor tRNA efficacy is optimized by modulating tRNA body sequences to individually fine-tune them to the physico-chemical properties of the cognate amino acid. suppressor tRNA had no discernible readthrough at endogenous native stop codons as determined by ribosome profiling. At clinically important PTC in cystic fibrosis transmembrane conductance regulator (CFTR), the suppressor tRNAs reestablished expression and function in cell systems and patient-derived primary cultures of nasal epithelia and restored the airway volume homeostasis. These results provide the framework for development of tRNA-based therapeutics with high molecular safety profile and high efficacy in targeted suppression of PTCs.

This chapter contains the results of collaborative effort of multiple groups and co-authors; Eric. J. Sorcher, Disha Joshi, Candela Manfredi at the Department of Pediatrics, Emory University School of Medicine, Atlanta, USA, Steven M. Rowe and Susan E Briket from Pulmonary, Alergy and Critical Care Mdicine, University of Alabama, USA. The development of suppressor tRNAs was done by Suki Albers from our group at University of Hamburg, Germany. Marcos Davyt, Miguel Angle Delgado-Toscano and I took part in designing, conducting and analysing the deep-sequencing experiments, which were analyzed bioinformatically by Leonardo Santos. I also analyzed the readthough efficiency on full-length CFTR summarized in Figure 5.1(e), Figure 5.4(a), (b) and (d), Figure 5.5, Figure 5.6 (b), (c) and (d). This study has been submitted for publication; the Chapter contains only part of the publication, my contribution along with the studies to optimize suppressor tRNAs, which I tested on rescuing expression and activity of full-length CFTR..

5.1.1 Repurposing strategy for human suppressor tRNA

Harnessing functionally conserved features of natural tRNAs and modulating sequences outside the anticodon, we successfully repurposed bacterial tRNAs to incorporate exclusively alanine at the UGA stop codon with codon: anticodon interactions resembling the Watson-Crick geometry of a sense-codon decoding tRNA (97). We reasoned that applying similar strategy and modulating human tRNA sequences that are crucial for tRNA's function in translation, e.g., the anticodon (AC)-stem and loop (Fig. 5.1a), which modulate accuracy of decoding, and the TΨC-stem that determines binding affinity to the elongation factor (118–120) we will enhance suppressor tRNA efficacy to decode a PTC. We also leveraged a synthetic lipid nanoparticulated system (121) to encapsulate in vitro transcribed suppressor tRNA and produce safe RNA-based therapeutics with high efficacy in PTC suppression in vivo and good molecular safety profile.

To repurpose human tRNAs to decode PTCs, we chose three human tRNASer, tRNAArg and tRNAGly families, which decode codons that are frequently mutated to PTCs (122). We first exchanged the anticodon of tRNASerUGA/tRNASerAGA, tRNAArgUCU and tRNAGlyUCC to UCA to pair to the UGA stop codon, creating the first generation tRNAsSup, tS, tR and tG, respectively (Fig. 5.1a,). The engineered suppressor tRNA variants were in vitro transcribed (IVT) with functionally homogenous 3' ends and their decoding efficiency was tested by co-transfecting them in human Hep3B cells with a plasmid-encoded PTC reporter of firefly luciferase (FLuc, Fig. 5.1b); the FLuc coding sequence was extended at its 5' end by 15 codons representing the context of the most common PTC (R208X-FLuc) in tripeptidyl peptidase 1(TPP1) gene associated with the autosomal recessive progressive lysosomal disorder, late infantile neuronal ceroid lipofuscinosis (CLN2). As expected, the anticodon-repurposed tS, tR and tG exhibited low readthrough activity with tR showing the highest efficiency (Fig. 5.1.c), likely because the natural tRNAArgUCU – the precursor of tR – is intrinsically prone to miscoding (123). To achieve similar decoding efficiency among all natural tRNAs, their sequences have been idiosyncratically finetuned to the chemical nature of the cognate amino acid, whereby the destabilizing thermodynamic effect of some amino acids is compensated by stronger interactions of the elongation factor with the TΨC-stem and vice versa, to achieve similar decoding efficiency among all tRNA isoacceptors (124). The three tRNA families we have chosen, are aminoacylated with serine, arginine or glycine, and these three amino acids span the entire spectrum of thermodynamic contributions (i.e., glycine is destabilizing amino acid, serine stabilizing and arginine nearly neutral (124). To enhance the efficiency in decoding PTCs, tS, tR and tG were subjected to a comprehensive set of sequence changes in the TΨC-stem for stabilization and AC-stem for accuracy in decoding (124,125), thereby preserving the recognition signals for their cognate aminoacyl-tRNA-synthetases (Fig 5.1a).

The energy contribution of different base pairs in stabilizing TΨC-stem interactions with the elongation factor (positions 49-65, 50-64 and 51-63, Fig. 1.1a) has been determined for prokaryotes (124). The eukaryotic (eEF1A) and bacterial (EF-Tu) elongation factors share conserved sites of aminoacyl-tRNAs binding (126), thus, we estimated the binding energy of the TΨC-stem modified variants to eEFA1 (Fig. 5.1a, table), using the values for prokaryotic counterpart (124). Position-specific changes in either AC-stem (Ai variants) or TΨC-stem (Ti variants) enhanced the readthrough activity of tS, but the simultaneous modulation of both AC-stem and TΨC-stem displayed the most robust effect (e.g., variants tSA1T5 and tSA2T5, Fig 5.1c). The tS variants with TΨC-stem less stably interacting with eEF1A (e.g., tST2 and tST5) exhibited higher suppression efficacy than the tST6 variant which is the most stably interacting with eEF1A (Fig. 5.1b, table).

Suppression efficacy enhancement of repurposed suppressor tRNA charged with serine – a stabilizing amino acid. (124) – was achieved by modest stabilization of the interactions with eEF1A. Arginine bears nearly no thermodynamic contribution to the aminoacyl-tRNA stability (124). tR variants with substitutions in the TΨC-stem, that would stabilize the interactions with eEF1A, exhibited higher readthrough activity (tRT6>tRT5=tRT8>tRT9), whilst changes within the AC-stem alone (tRA2) or in combination with the TΨC-stem (tRA2T5) markedly reduced the PTC rescue (Fig. 5.1c). Glycine is a destabilizing amino acid (124), however mutations in TΨC-stem stabilizing the interactions with eEF1A (tGT6) only marginally enhanced the tG readthrough activity. Overall, the tG variants showed much lower readthrough activity compared to tS and tR variants, likely owing to the intrinsic hyper accuracy of natural tRNAsGly (123). Yet, for some PTCs this might be still sufficient to potentially address diseases in which the therapeutic threshold is low, such as cystic fibrosis (CF) (127). Together, our findings indicate that to repurpose native tRNAs to decode PTCs, unique design principles should be established for each tRNA family tailored to the affinity for the elongation factor and chemical nature of the cognate amino acid.

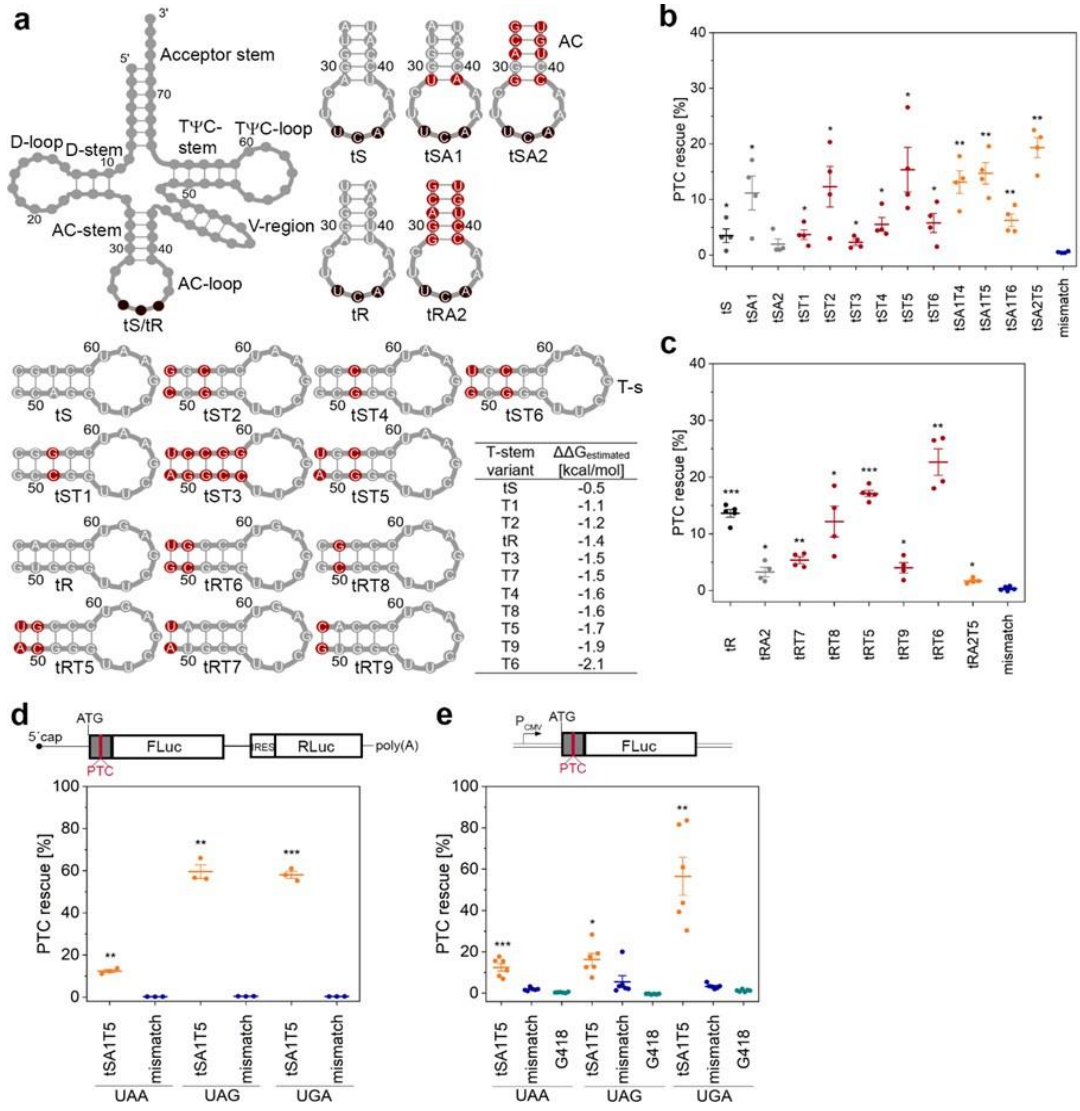

Figure5.1 :tRNA variants to decode different PTCs at Ser (tS) and Arg (tR) codons.

a, tRNA cloverleaf structure (left) with tRNA regions designated. Nucleotide substitutions in the AC stem (Ai variants) or TΨC-stem (Ti variants) of tS or tR are highlighted in red. Table, estimated ΔΔG° values for binding affinities of eEF1A to the TΨC-stem**. b, c** Suppression of UGA PTC in human liver Hep3B cells with tS (b) or tR (c) variants monitored with R208X-FLuc and normalized to wildtype FLuc. tS and tR, black; AC variants, grey; TΨC-stem variants, red; AC- and TΨC-stem variants, orange; mismatch tRNA, dark blue. d, e, tSA1T5 targets PTCs with different stop codon identities. Suppression activity monitored by co-transfecting in vitro transcribed tSA1T5 with FLuc-R208X-RLuc mRNA in murine liver Hepa 1-6 cells **(d)** and with S446X-FLuc plasmid DNA in bronchial epithelial Suppressor tRNA cells **(e)** and normalized to wildtype (WT-)FLuc. G418, low-molecular readthrough agent geneticin (cyan). *P < 0.05, **P < 0.01, ***P < 0.001 compared to the corresponding mismatch tRNA (one-sided t test).

5.1.2 Assessing suppressor tRNA efficiency at three different PTCs

We next assessed the PTC rescue efficacy for the three different stop codons, as pathogenic nonsense mutations occur for all three PTCs (e.g., UGA – 38.5%, UAG – 40.4% and UAA – 21.1% frequency) (122). In the screening process, along with the CLN2 disease-associated R208X PTC, we considered a pathogenic mutation (S466X) in CFTR implicated in CF; this mutation provides another disease-relevant PTC context and in CF patients occurs with different stop codon identities (https://cftr2.org/). At an optimal suppressor tRNA concentration, which does not alter cell viability (Fig5.2), tSA1T5 suppressed both UGA and UAG PTCs with much higher efficiency than UAA (Fig. 5.1d. Notably, tSA1T5 was markedly more efficient at all PTCs with three different stop codon identities than the known readthrough compound G418 (Fig. 5.1d). The efficacy of tSA1T5 at the UGA PTC was greater for the S466X than for R208X (Fig. 5.1d vs. 1.1c), suggesting that the PTC sequence context also modulates readthrough efficiency – an effect that has been reported for aminoglycosides-stimulated readthrough at natural termination codons (128).

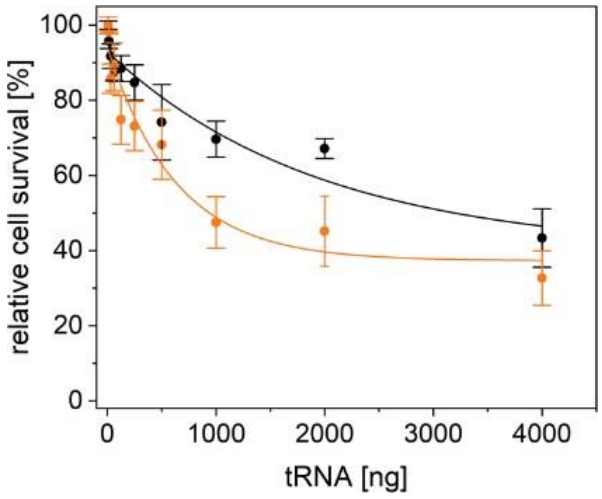

Figure 5.2: Dose dependent cell viability with suppressor tRNA transfection Cell viability assay 24 h post transfection of Suppressor tRNA cells transfected with different tS (black) and tSA1T5 (orange) concentrations. The signal was normalized to mock-transfected cells; the signal with the lowest tRNA concentration was set as 100%. Data are means ± SEM (n=3 biologically independent experiments)

5.1.3 Toll-like receptors are marginally activated by suppressor tRNA.

Next, we assessed whether the engineered suppressor tRNA stimulates mammalian innate immune response through activation of human Toll-like receptors (TLRs), and specifically TLR7 and TLR8 which are augmented by synthetic and viral RNA. In human TRL-transformed

HEK293 cells, the suppressor tRNA did not activate TLR7 and only marginally TLR8, however, to the extent of the mock transfection (Fig. 5.3), suggesting that it might be an unspecific effect.

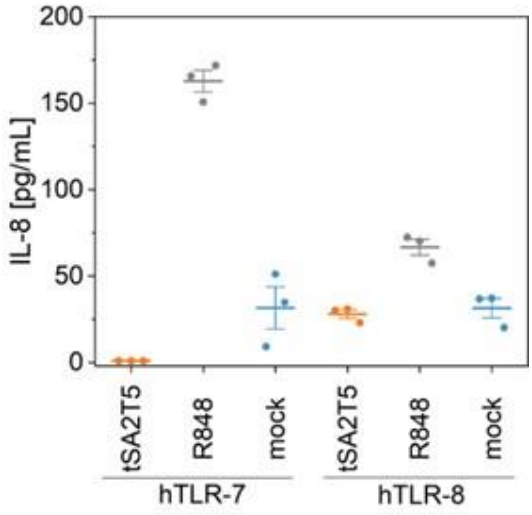

Figure 5.3: Immune activation by suppressor tRNA in cell culture. TLR-dependent activation by tSA2T5 monitored in HEK293 cells stably expressing human TLR7 and TLR8 receptors. R848 (grey), activated both TLR7 and TLR8 and served as a positive control; mock (blue) transfected cells. Data are means ± SEM (n=3-6).

5.1.4 Suppressor tRNA restores the expression of full-length CFTR protein harboring PTC mutations in cell culture model.

We addressed the efficacy of the nonsense suppressor tRNAs to restore expression of the full-length CFTR protein harboring different pathogenic mutations in cell models. PTC-tailored suppressor tRNAs were specific to the PTC identity and context and rescued full-length S466X-CFTR (X=UGA or UAA) or R553X-CFTR (X=UGA) transiently transfected in CFBE41o− cells (Fig 5.4a and 5.4b). Engineered suppressor tRNAs with modified TΨC- or AC-stem sequences (e.g. tSA1T5, tSA2T5, tRT5, tRT6) exhibited higher efficacy in rescuing full-length CFTR expression than the variants with exchanged anticodon only (i.e. tS and tR, respectively; Fig. 5.4a 5.4b). S466X is a CFTR mutation naturally present in CF patients as both PTC identities UGA or UAA. Although the suppression efficacy at the UAA PTC was slightly lower than at UGA PTC both tSA1T5 and tSA2T5 efficiently suppressed the most refractory stop codon to suppression (UAA). tRT5 rescued R553X-CFTR expression to 22% of that of the WT-CFTR (Fig. 5.4d); the nearly equal mean coverage of the ribosome profiling spectra up- and downstream of the PTC is indicative of no substantial ribosomal drop-off at the PTC (Fig. 5.4d). Quantification of the transepithelial ion transport in Fischer rat thyroid (FRT) cells revealed that both tR and tRT5 substantially rescued R553X-CFTR channel activity, with tR5 being more

effective than reaching appr. 10% of the WT-CFTR activity (Fig. 1.4c). Note that the uniform ribosome coverage (i.e., the nearly equal mean coverage of the ribosome profiling spectra) up- and downstream of the PTC is indicative of no substantial ribosomal drop-off at the PTC (Fig. 1.4d).

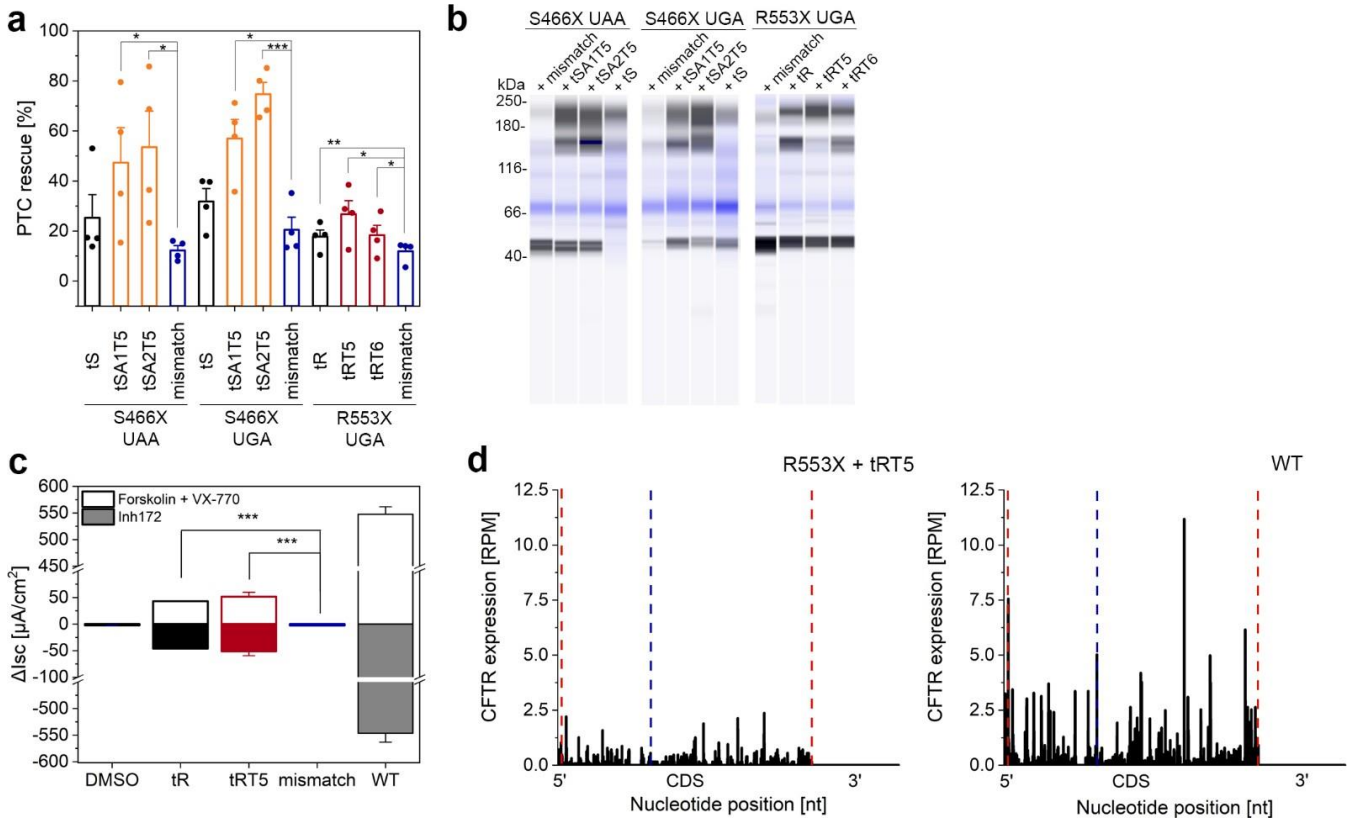

Figure 5.4: PTC suppression and restoration of CFTR function in cell model a, Efficacy of tS and tR variants in restoring expression of S466X(UGA)-CFTR, S466X(UAA)-CFTR or R553X(UGA)-CFTR in Suppressor tRNA cells monitored by band C expression normalized to that of WT-CFTR. Data means ± SEM (n=4). *P < 0.05, **P < 0.01, ***P < 0.001 compared to the corresponding mismatch tRNA (one-sided t test). **b,** Suppression activity in full-length CFTR was monitored by automated immunoblotting (JESS system) using monoclonal CFTR-NBD2 antibody (1:100 dilution, #596) in Suppressor tRNA cells co-transfected with plasmid-encoded S466X(UGA)-CFTR, S466X(UAA)-CFTR or R553X(UGA)-CFTR and the corresponding in vitro transcribed tRNA suppressor. **c,** short-circuit current (ΔIsc) of R553X-CFTR expressing FRT monolayers transfected with tR or tRT5 and compared to WT-CFTR. Forskolin, CFTR activator (green); VX-770, potentiator (ivacaftor; light grey), Inh-172, CFTR inhibitor (dark grey). Data means ± SEM (n=3-5). **d**, Ribosome density profile of tRT5-rescued R553X-CFTR mRNA (total expression, 27 RPKM) compared to WT-CFTR (129 RPKM) in Suppressor tRNA cells. Red dashed lines, start and stop of CFTR CDS; blue dashed line, fist nucleotide of the UGA PTC.

5.1.5 Suppressor tRNA does not enhance readthrough at native stop codons beyond natural background level.

To assess potential off-target effects of suppressor tRNAs on native stop codons, we subjected ribosome profiling of Suppressor tRNA cells expressing R553X-CFTR and treated with tRT5::UGA. The readthrough frequency at canonical stop codons was determined using the ribosome readthrough score (RRTS), which is defined as a ratio of the mean read density over the coding-sequence and the mean read density between the natural termination codon and next in-frame stop codon in the 3'UTRs. Out of > 10,000 transcripts detected we detected readthrough events at the canonical UGA stop codons of a handful transcripts, which was comparable to the readthrough at UGA codons in controls, (Note that different number of genes with internal UGA stop codons were detected as expressed in Suppressor tRNA and only transcripts detected in both replicates and the control were considered). (Fig. 5.5).

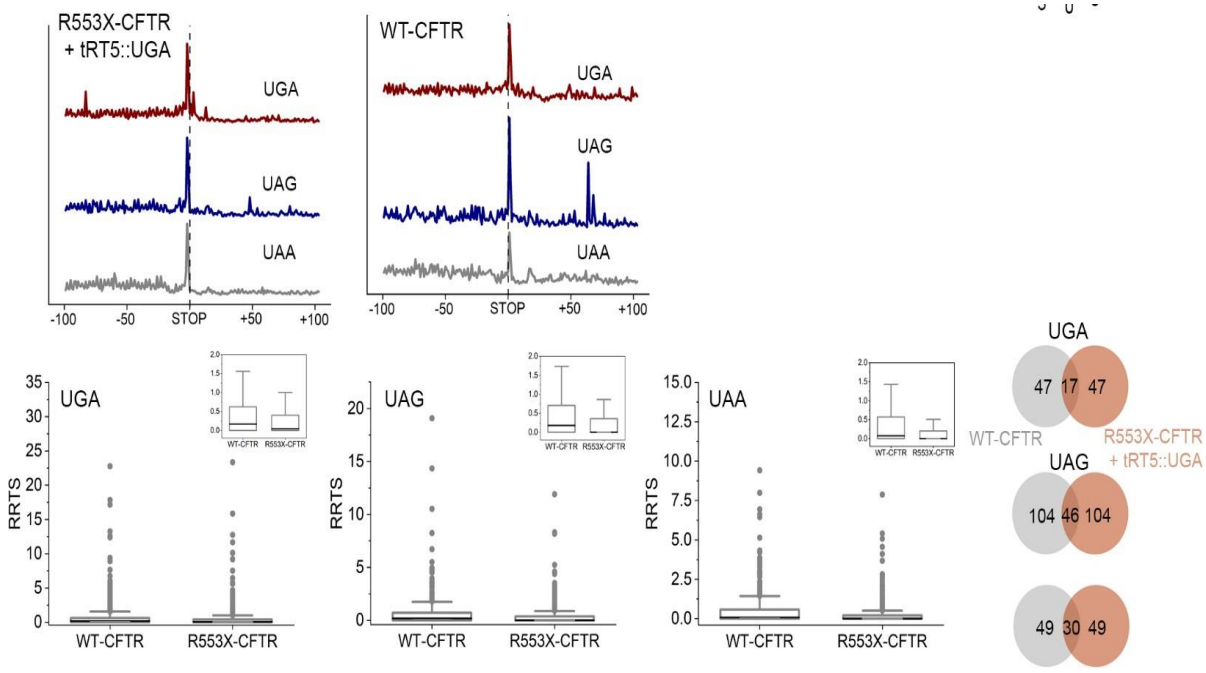

Figure 5.5. Suppressor tRNAs do not induce readthrough at native UGA codons in cell culture., Very low readthrough at all three natural stop codons (including the unspecific ones UAA and UAG not targeted by the suppressor tRNA) detected in the cumulative coverage plots (upper panels), the ribosome readthrough score (RRTS, lower panels). Suppressor tRNA cells expressing WT-CFTR., replicate #1 and #2. The RRTS is a comparison between tRNA-treated samples compared to WT-CFTR expressing Suppressor tRNA cells. We noted that all detected transcripts with a high RRTS (Venn diagrams) are within 10%ile of genes with highest expression level, suggesting a high proportion of false positives.

Even at transcript internal UGA sites that are naturally selected for high readthrough efficiency, we detected no readthrough enhancement beyond the natural background level. Notably, this

readthrough frequency was also comparable to that at the other two stop codons (UAA and UAG) not targeted by the suppressor tRNAs, with little to no overlap of the transcripts with the untreated control samples, suggesting that our tRNA suppressors exhibit no specific adverse effect and do not enhance the readthrough at native stop codons beyond the natural stochastic background readthrough level.

5.1.6 Suppressor tRNA stabilizes CFTR mRNA and restores full-length CFTR expression in patient-derived primary cells.

Given the susceptibility of nonsense mutation-containing native mRNAs to nonsense mediated mRNA decay (NMD) (129,130), we next tested the effect of our suppressor tRNAs on full-length CFTR (i.e. with all introns and exons) in gene-edited bronchial epithelial cell line (16HBEge) endogenously expressing PTC-CFTR (R1162X/-) and in a primary human nasal epithelial cells (hNE) obtained from a CF-patient homozygous for R1162X/R1162X. In the proliferating 16HBEge cells, tRNA remained stable for at least 72h (Fig. 5.6a). tRT5 alone markedly stabilized the full-length CFTR mRNA expression to a level comparable to the NMD inhibitor alone (Fig. 5.6b). Combined treatment with tRT5 and NMD inhibitor synergistically augmented mRNA level two-fold (Fig. 5.6b), but in both 16HBEge and primary hNE cells only marginally enhanced the full-length CFTR protein (band C) expression compared to the tRT5 alone (Fig 5.6c, d). For comparison, PTC124 (ataluren) clinically approved in Europe for treatment of Duchenne muscular dystrophy and previously shown to cause readthrough at PTCs (131,132), although alone stabilized the CFTR mRNA, did not enhance protein expression (Fig. 1.6b, c). In primary hNE cells, tRT5 alone augmented CFTR channel activity by approximately two-fold over the background recordings with mismatch tRNA (Fig. 5.6e). Combined treatment with tRT5 and NMD inhibitor did not increase further the transepithelial currents (Fig. 5.6e), mirroring the effect on full-length protein expression (Fig. 5.6d). We noted alterations of hNE viability upon prolonged treatment with NMD inhibitor (i.e., 24 or 48h), hence combined treatments in patients may cause adverse effects (133).

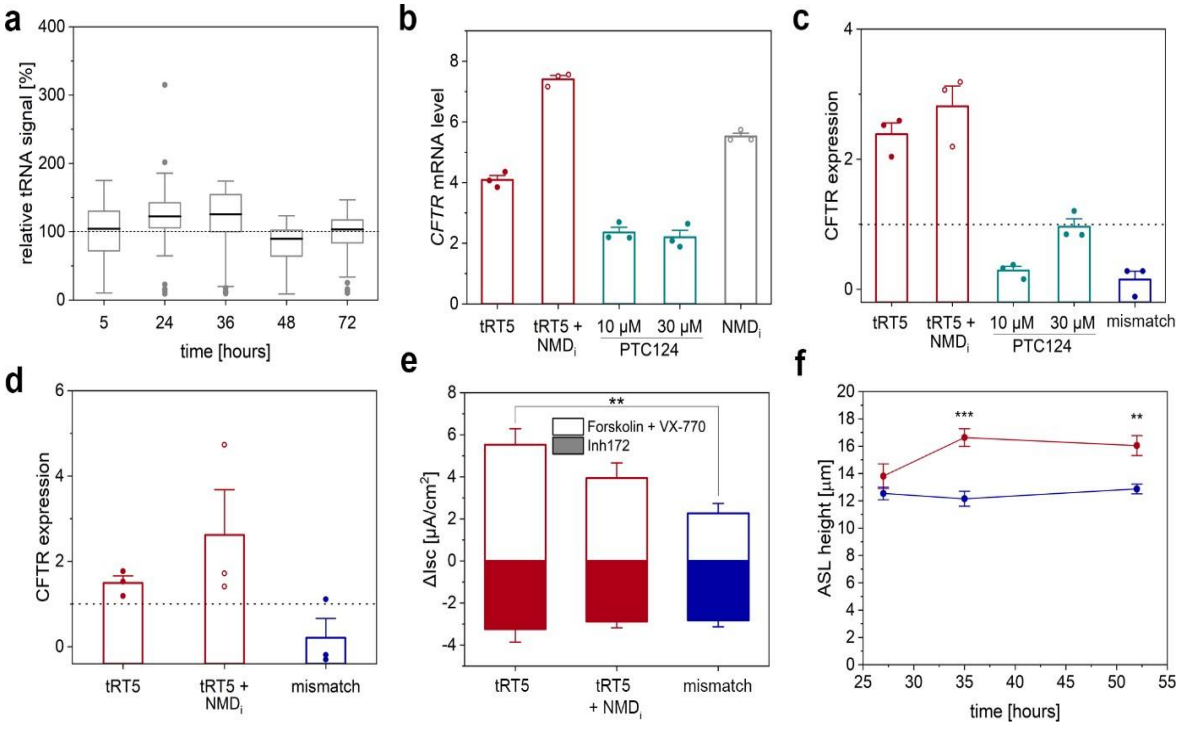

Figure 5.6: PTC suppression and restoration of CFTR activity in 16HBEge cell line and patient-derived hNE cells. **a,** tRNA suppressor stability in gene-edited 16HBEge cells monitored with tRNA-specific microarrays (n=2 independent replicates) and normalized to the mean of the signal at first time point (5h) post transfection set as 100 % (horizontal line). **b, c**, tRT5 efficacy alone or by co-treatment with NMD inhibitor compared to treatment with PTC124 or mismatch tRNA in augmenting expression of CFTR mRNA **(b)** or R1162X-CFTR (band C, c) in 16HBEge cells (R1162X/-; X=UGA). mRNA expression fold-changes comparison to untreated cells **(b).** Band C fold-change comparison to cells transfected with mismatch tRNA and treated with NMDi (dashed line, c). **d,** tRT5 efficacy alone or by co-treatment with NMD inhibitor compared to treatment with mismatch tRNA (blue, closed circles) in augmenting expression of R1162X-CFTR (band C) in primary hNE (R1162X/R1162X; X=UGA) cells. Fold-change comparison to treatment with mismatch tRNA and NMD14 (dashed line). Data means ± SEM (n=3). **e,** Short circuit current (ΔIsc) measurements (Ussing chamber) of R1162X-CFTR suppressed with tRT5 alone or combined with NMD inhibitor compared to mismatch tRNA. Forskolin, CFTR activator andVX-770, potentiator (ivacaftor; white), Inh-172, CFTR inhibitor (dark grey). Data means ± SEM (n=8). **f,** ASL volume measurement of hNE (R1162X/R1162X) cotransfected with tRT5 (red) or mismatch tRNA (blue). Data are means ± SEM (n=5). ** P=0.0061, *** P=0.0002 (two-way ANOVA with Sudak's multiple comparisons)

5.2 Sequence context and ribosome collisions affect suppressor tRNA efficacy and readthrough at PTCs

In this chapter, I elucidate why nonsense suppressor tRNAs, in particular the variants introduced in chapter 1, have variability in their PTC suppression efficiency. This work also aims to understand which different factors or features affect this variability. Furthermore, the suppressor tRNAs, as shown in chapter 1, did have almost no unspecific effects on natural termination codon, thus here we also address the specificity to PTCs. CFTR gene is chosen as the disease model for this study due to possibility of examining multiple possible PTC mutations within the same mRNA molecule. Overall, we shed light on different factors that influence PTC suppression by engineered nonsense suppressor tRNAs and provide a new twist in previously described sequence context influence on PTC rescue.

This chapter contains results of collaborative effort, and it is prepared for publication that will have multiple co-authors: I took a lead on this study and designed, conducted and analyzed the majority of the experiments. Some experiments were done in collaboration with Marcos Davyt, Miguel Angel Delgado-Toscano, Alejandro Jimenez-Sanchez. The bioinformatic analysis for ribosome speed studies was done in collaboration with Leonardo Santos. Eric. J. Sorcher, at the Department of Pediatrics, Emory University School of Medicine, Atlanta, USA, was responsible for providing Calu3 W1282X and Calu3 parental WT cells. The development of suppressor tRNAs (also in Chapter 1) was done by Suki Albers from our group at University of Hamburg, Germany.

5.2.1 CFTR PTC mutations serve as model system for assessing context dependence of PTC rescue by non-sense suppressor tRNA.

We addressed the efficacy of CFTR PTC rescue with non-sense suppressor tRNA in chapter 1. We demonstrated that CFTR mutations can be rescued in patient derived nasal epithelial cells along with other cell culture models. All these studies were tested on various PTC mutations with various stop codons. Notably variation in rescue was observed, this variation for mutations with similar stop codon identities could only be an intrinsic feature of the stop codon location in the sequence of the mRNA. We then investigated the origin of this variability, for this we chose again CFTR as a model system, ideally because of multiple possibilities of PTC mutations on same mRNA. CFTR is known to have more than 70 possible PTC mutations (Figure 5.7 A) (https://cftr2.org/). To test this, the luciferase reporter system explained earlier in chapter 1 was

utilized. A readthrough assay was designed for CFTR PTC mutations, based on their prevalence in population with most common PTCs with UGA stop codon (G524X, W1282X and R553X) and with the least common PTCs that can present them with UGA, UAG or UAA stop codon (S466X, W1204X or W846X). Readthrough efficiency was tested by co-transfecting suppressor tRNA with a plasmid encoded PTC reporter of firefly luciferase (Fluc) which was extended by the context of the PTC with 7 codons on either side of PTC mimicking the 3' and 5' context of the natural PTC in CFBE41o- cell line (Figure 5.7 B). To keep the number of variable factors low in the study we choose human tRNASer suppressor tRNA of all generations tS, tSA1T5 and tSA2T5 which are tRNASer generation 1, generation 2 and generation 3 respectively (as explained in chapter1) and will be named as GEN1, GEN2 and GEN3 hereon. All the suppressor tRNA had respective anticodon UGA, UAG or UAA when testing readthrough efficiency with reporters harboring same PTC mutations respectively.

Nonsense suppression of suppressor tRNA GEN1, GEN2 and GEN3 were assessed with the Fluc reporter system assay (figure 5.7C), as was expected GEN3 tRNA had higher rescue of readthrough when compared to mismatch tRNA, all normalized to WT Fluc expression. For UGA PTC mutations (prevalent CFTR mutations) W1282X had the highest rescue when compared G542X and R553X PTC mutations also with UGA PTC identity. Within the same PTC identity (UGA) rare mutations S466X, W846X and W1204X had relatively lower rescue compared to the prevalent mutations. This variation alone is an indication that sequence context was influencing how rescue of same stop codon identity with same nonsense suppressor tRNA. Along, with accessing variability of rescue within the same PTC, we also tested for variability with PTC identity, Fluc reporter with context of S466X, W846X and W1204X respectively with other stop codon identities UAG and UAA were also tested against same GEN1, GEN2 and GEN3 nonsense suppressor tRNA with respective anticodons. As it is already known that UAA PTC mutations are the most pervasive when it comes to suppression, our results from Fluc reporter assay matched the common understanding with UAG carrying Fluc reporter having lower rescue compared to UGA and UAA with the least rescue.

5.2.2 Comparing influence of 3' and 5' PTC sequence context on its rescue by nonsense suppressor tRNA

To assess the impact of sequence context on nonsense suppressor tRNA suppressibility we decided to look at the sequence context as separated 3' context and 5' context. Based on studies earlier that were done to understand the influence of sequence context on PTC suppression with aminoglycoside, we generated an ideal sequence context both upstream and downstream of PTC

mutation (Figure 5.8A). The ideal sequence context was summation of all the known nucleotide identities in 5' and 3' direction of PTC which has the most influence in its suppression, ideally allowing the most rescue. In 3' direction the first nucleotide that had the most influence was C at +4 position then followed by A at +5 position and then A at +6 position, +7 position was rarely found to have influence in literature hence here we took C then followed by U at +8 position and A at +9 position when the first nucleotide of PTC is depicted as +1. In 5' direction the first nucleotide was A at -1 position followed by A at -2 position then followed by C at -3 position then at -4, -5 and -6 we took A, A and C respectively when the first nucleotide of PTC is depicted as +1. We then took all the CFTR PTC mutations shown in figure 5.7 A, then compared the upstream and downstream region of the PTC mutation with the ideal sequence contexts upstream and downstream region respectively to see which mutations' sequence context in the most and least similar to the ideal sequence context. The similarity was divided into three groups of 0-30%, 30-60% and 60-100% similar for both upstream and downstream separately as shown in figure 5.8 B.

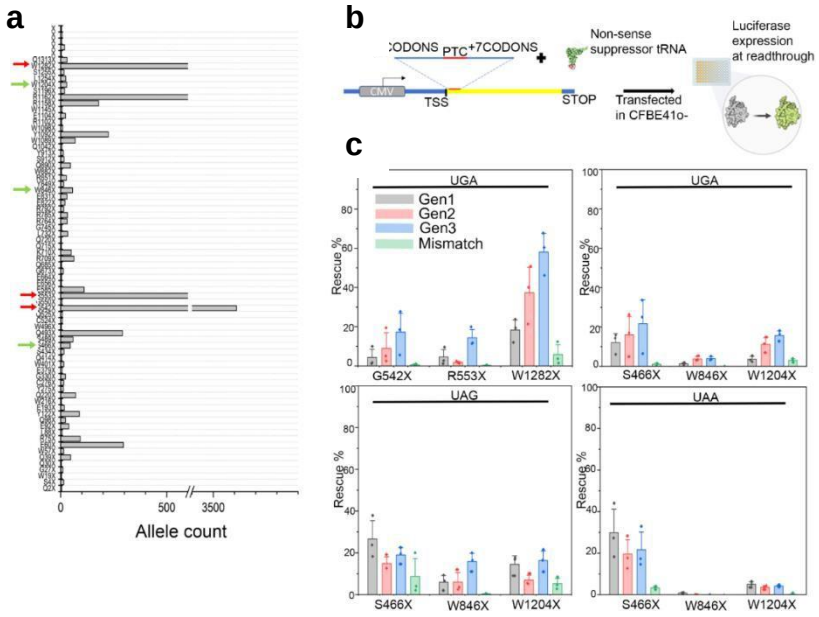

Figure 5.7 : **CFTR has more than 70 mutations (https://cftr2.org/.)** A) Here shows the prevalence/allele count of different PTC mutations in CFTR gene from 89,000 patients. Mutations with red arrows are prevalent and with green arrows are rare mutations. B) schematic of model system, firefly luciferase reporter system embedded in PGL45.1 plasmid driven by CMV promoter where a 15 codon context with PTC in middle is inserted right after translation start site (TSS), for readthrough assays plasmid was transfected in CFBE41o- cells with suppressor tRNA, expression of luciferase in 96 well plate reader was the output. C) readthrough of prevalent and rare CFTR mutations with GEN1, GEN2 and GEN3 tRNA, which are tRNASer body-based suppressor tRNA. Top left, readthrough of prevalent mutations R553X UGA, G542X UGA and W1282X UGA. Top right, bottom left and right readthrough of rare mutations S466X, W846X and W1204X, where each sub panel is UGA, UAG and UAA respectively.

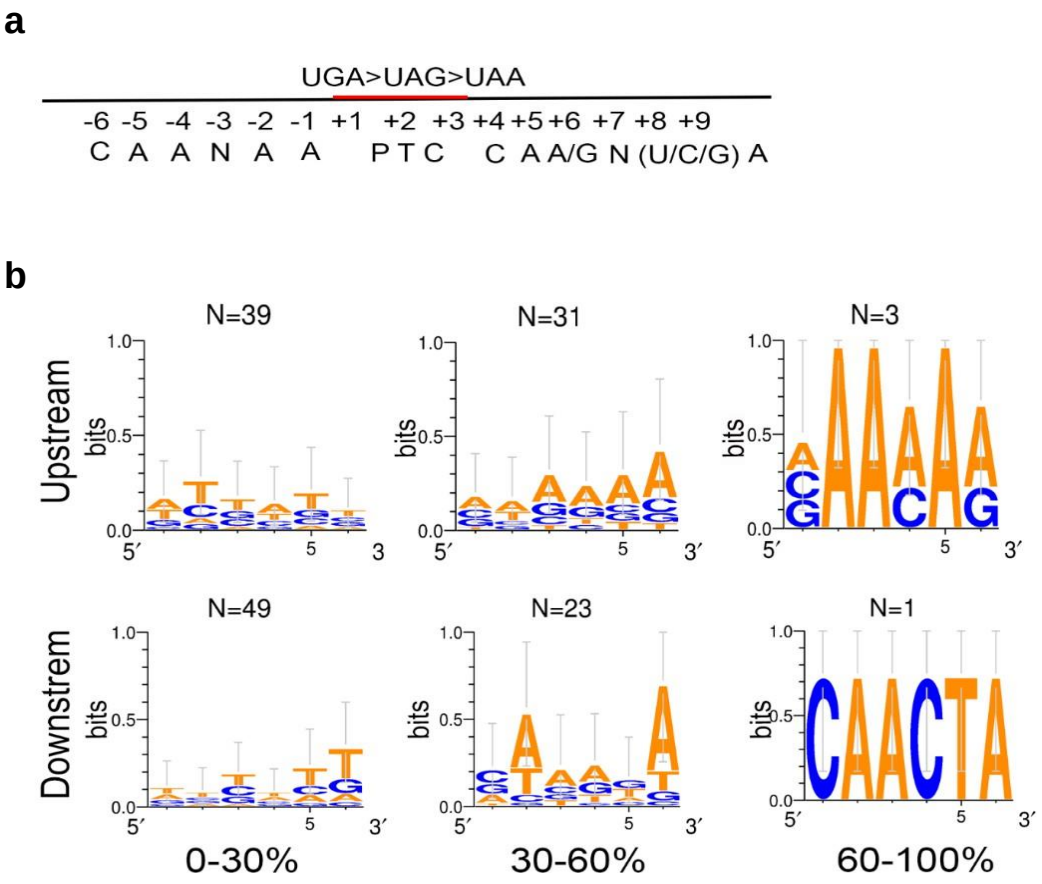

Figure 5.8 : Ideal readthrough sequence A) ideal sequence generated from multiple articles (128,134,135) that studied nucleotide wise influence on readthrough when corrected by aminoglycosides, along with suppression ability of stop codon identity from high to low UGA>UAG>UAA. B) sequence logo designed on Weblogo3® for all PTC mutations in CFTR, and segregated based on their percentage similarity to the ideal sequence in three groups 0-30%, 30-60% and 60-100% for upstream and downstream sequence context of all the PTC mutations, 'N' represents number of mutations falling in each category

Table 5.1: list of mutations selected in each category.

UGA	**% similarity**	**Upstream**	**Downstream**
	0%	R1162X	R1162X
	17%	W1282X	W846X
	33%	G542X	R553X
	67%	C524X	W1282X
UAG	**% similarity**	**Upstream**	**Downstream**
	0%	S489X	Y122X
	17%	Q715X	S466X
	33%	S466X	E585X
	67%	Q1411X	Q685X
UAA	**% similarity**	**Upstream**	**Downstream**
	0%	Q493X	Y275X
	17%	W846X	E60X
	33%	E813X	W57X
	67%	N/A	N/A

We then assessed the individual effect of downstream and upstream context of different CFTR PTC mutations with all different stop codon identity respectively, a few PTC mutations from each category of similarity percentage were selected for UGA, UAA and UAG mutations as shown in table 2.1. Their suppression was tested with the same Fluc reporter system in CFBE4o- cells, when transfected along with GEN3 tRNA only. We decided to go with GEN3 tRNA as from figure 5.7C we observed that variability was higher in GEN3, and rescue was to a greater extent which makes it easy to visualize changes. From here on in the study we only tested PTC suppression with GEN3 tRNA. When we assessed the readthrough for all the selected PTC mutations and overall upstream context had a slightly greater influence towards when using GEN3 suppressor tRNA, W1282X UGA upstream context had the greatest influence, with S489X UAG, E585X UAG and Y275X UAA showing similar pattern. This was not the case

always as for mutations Q685X UAG, Q1411X UAG, E813X UAA and E60X even with increase in upstream context similarity to ideal sequence, the readthrough by GEN3 suppressor tRNA was not increased. Downstream context had little to no influence in how PTC readthrough occurred with GEN3 suppressor tRNA. (Figure 5.9)

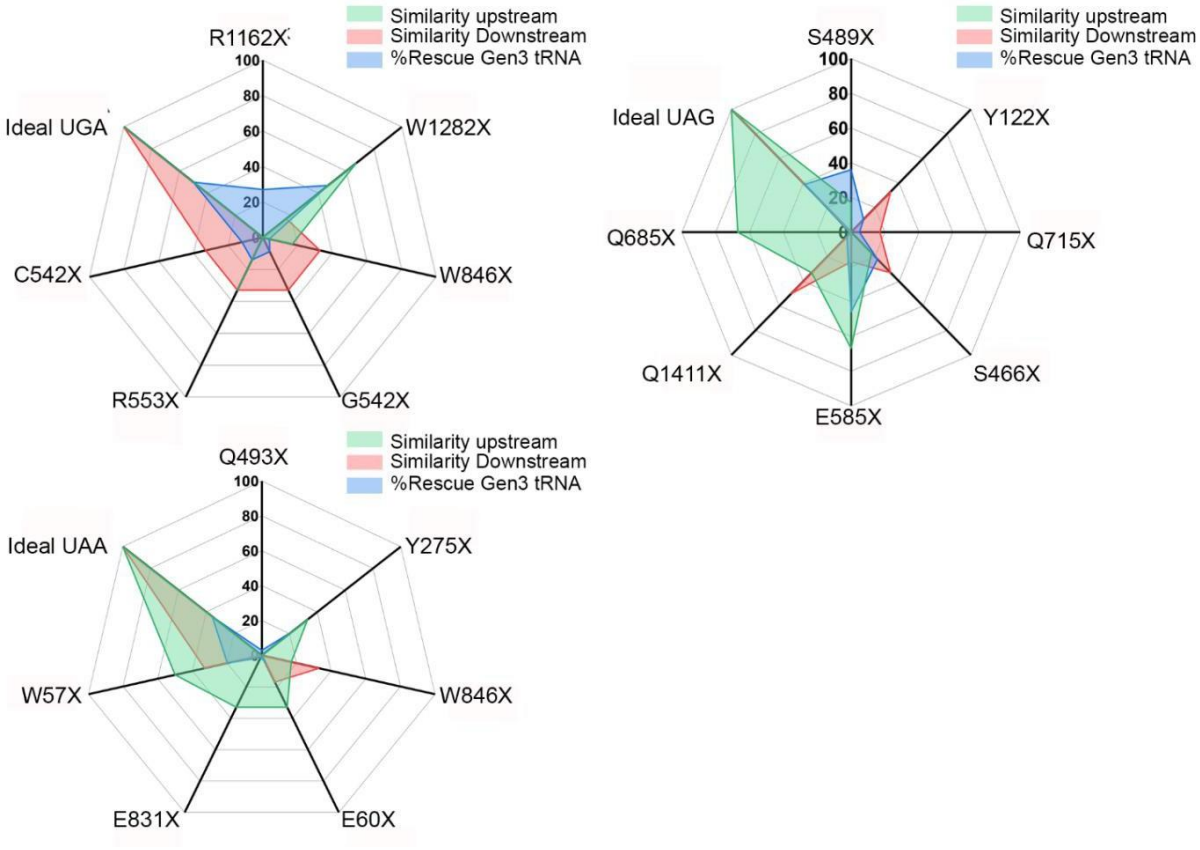

Figure 5.9: Readthrough based rescue of selected PTC mutations by GEN3 suppressor tRNA. Clockwise from top left UGA, UAG and UAA, spider plot representing relationship between sequence similarity of upstream (green) and downstream(red) context of PTC mutations (UGA, UAG and UAA respectively) to ideal sequence and their readthrough(blue) using Fluc reporter system by GEN3 suppressor tRNA.

5.2.3 Ribosome speed at larger upstream sequence context affects PTC rescue when using nonsense suppresor tRNA

We understood how a short sequence context of a PTC influences its rescue when using suppressor tRNA by its upstream sequence than its downstream sequence. The shorter sequence context consisted of regions that could possibly interact with the ribosome stopping at the PTC site. As it is understood that PTC rescue with small molecules is fundamentally based on increasing the time for termination factors to bind and allow near cognate tRNA to rescue PTC. When we use suppressor tRNA on longer contexts such as R1162X UGA shown in chapter 1

had a greater rescue with a GEN3 tRNA when we compared it to a short sequence context, similar results can also be observed for S466X UGA and S466X UAA, also shown in chapter 1. Hence, we wanted to test how longer context could influence suppressor tRNA mediated rescue, if shorter context does not influence it greatly. To check for longer context influence, we calculated ribosomal occupancy in CFBE4o- cells for CFTR, based on the ribosomal occupancy we calculated ribosomal speed at codons by using inverse of occupancy since higher the occupancy slower is the decoding of the codon. We calculated upstream codon speeds upto 60 codons with an average of 5 codon interval for all CFTR PTC mutations sequence contexts. We used these 5 codon interval values from PTC to 60 codons upstream to generate an upstream speed profile for each mutation (Figure 5.10 A). We then made a summation of all the speed profiles and set threshold of deviation of speed from the median with maximum overall change and selected PTCs based on fold change threshold above 1.25 and under 0.75 (Figure 5.10 B), the selected PTCs were binned into three segments, where PTC upstream speed changed were close to PTC, between -5 to -35 codons, between -35 to -60 and with no overall change. We saw mutations such as R1162X UGA was segmented in the category of speed changes away from the PTC and W1282X close to PTC mutation Figure 5.10 C). To check if the W1282X mutations speed changes near the PTC affects rescue by nonsense suppressor tRNA, we used the Fluc reporter system where this time it was extended by 35codons upstream of PTC and 3 codons downstream of PTC, mimicking the longer W1282X PTC upstream sequence context. (Figure 5.11 A) We called this upstream elongated sequence context reporter system as extended W1282X, in the rescue with GEN3 tRNA it was approximately 40% lowly rescued when compared to short context W1282X, compared to mismatch tRNA normalized with WT Fluc expression as in figure 5.11 D. We also questioned if this is really due to sudden speed changed that happen near the PTC or is it because now the firefly luciferase is extended much longer and naturally has low expression leading to false lowering in readthrough of PTC. To check this, we induced changed on the upstream context region of W1282X such that the average codon speed is within the threshold we set earlier but not change the amino acid identity and called it as W1282X extended Δ (figure 5.11 B, C). We also checked an extended F.luc reporter which contained the same extended context of W1282X on the upstream region but with no PTC, which when compared to WT F.luc expression was only marginally reduced affirming any changes with W1282X extended PTC were not due to extended length of the reporter system. (Figure 5.11 D).

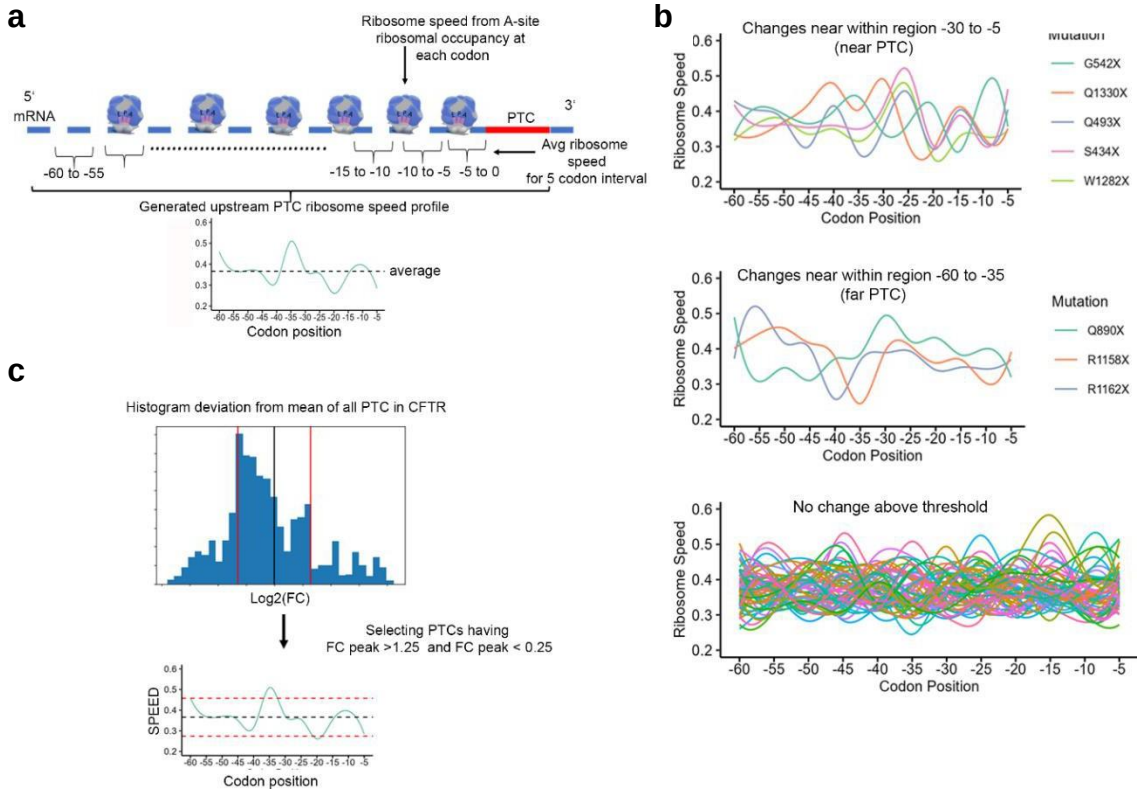

Figure 5.10: characterizing upstream codon speeds for all PTC, method schematic and speed plots for near and far PTC changes. A) schematic for calculating PTC upstream by using inverse ribosome occupancy values for each codon determined by ribosome sequencing on cfbe41o- cells, speed profiles were generated using 5 codon average speed of ribosome from PTC to 65 codons upstream of PTC. B) determining FC values for all the PTC mutations speeds profiles using a histogram deviating from mean, FC peak > 1.25 and FC < 0.25 with equal distance on each side was used to determine if the change in speed is true. C) All CFTR PTC mutations upstream speed changes were categorized into three different speed change positions from PTC, changes near PTC mutation or changes between PTC and upstream 35th codon, changes far away from PTC or changes between 35th upstream codon and 60th upstream codon and rest were binned in a separate category where no changes were observed

W1282X extended Δ, when rescued with GEN3 nonsense suppressor tRNA had an increase in rescue when compared to W1282X extended, indicating that sudden speed changes near the PTC affects how PTC is rescued using nonsense suppressor tRNA. (Figure 5.11 D)

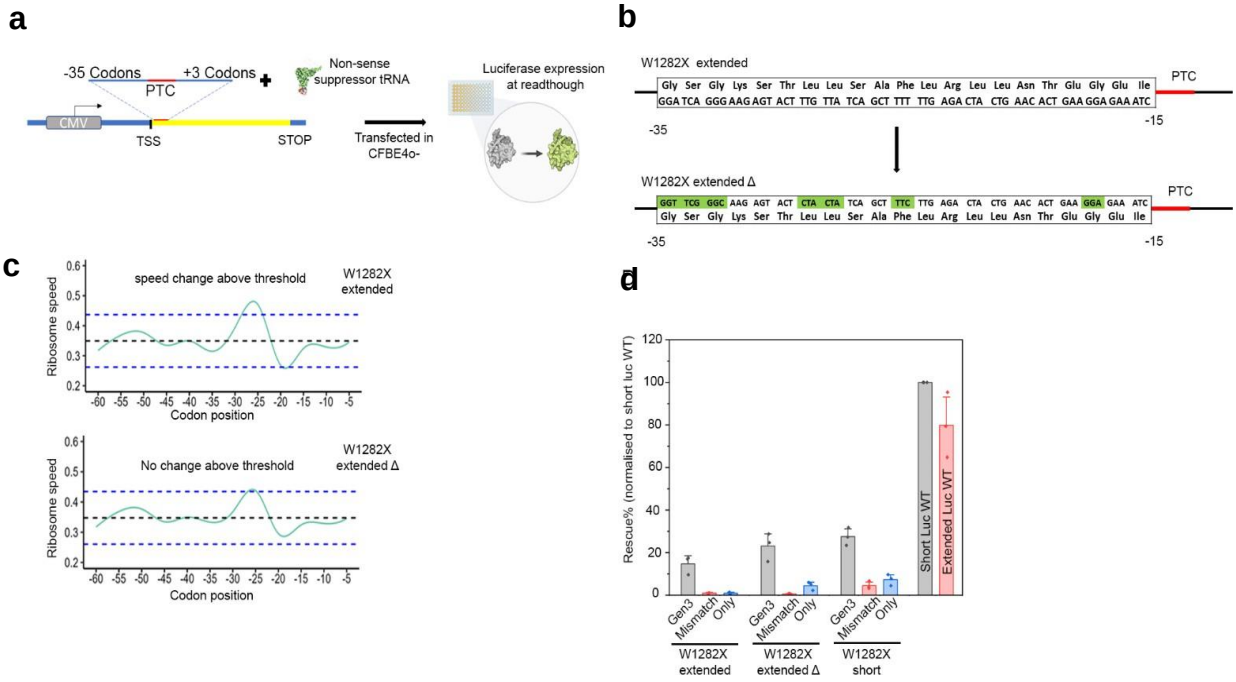

Figure 5.11 Generating longer PTC context for Fluc reporter assay, to determine influence of upstream codon speed change on PTC rescue by suppressor tRNA. A) schematic of 35codon long upstream sequence context of W1282X UGA PTC mutation as a Fluc reporter system embedded in PGL45.1 plasmid, transfected in cfbe41o- cells for readthrough assay of long upstream context of PTC mutations. B) schematic of change in codon sequence of W1282X extended codon context(green) to optimize speed without compromising the amino acid identity of the context called as W1282X extended Δ.C) FC plots for speed changes upstream of PTC for W1282X UGA PTC mutations, where W1282X extended Δ speed changes are within the set FC threshold value. D) Fluc based readthough assay for long upstream sequence context of W1282X extended, W1282X extended and W1282X short context (7 codon upstream), where with GEN3 treatment (grey) rescue is lowered for W1282X extended but then is regained when speed is optimized in W1282X extended Δ, when all were compared to mismatch tRNA treatment (pink) and only is no tRNA control (blue). All the samples were normalized to short context WT luciferase, also in comparison on how long extension of luciferase affects its expression with extended luc WT.

5.2.4 Collisions can be detected on W1282X CFTR mRNA in cell line models

We know that W1282X PTC mutation in CFTR is notoriously difficult to correct. We wanted to see whether this low correction on full length models can be attributed to the sudden speed changes near the PTC as we show earlier on reporter systems. For this we chose calu3 W1282X cell line system which has constitutive expression of CFTR mRNA with W1282X mutation and also the wild type (WT) cell line calu3 Parent with CFTR mRNA expression without PTC mutation gifted to us by Eric. J. Scorcher's lab. By this cell line model, we could see a fully

expressed CFTR mRNA which is processed naturally compared to a plasmid system. We ran ribosome profiles on a sucrose gradient 15%-60% on total cell lysates of both cell lines, we ran profiles directly from the lysates and RNase1 treated lysates, which would cleave any mRNA not protected by ribosomes. We saw a persistent disome peak in both calu3 Parent WT cells and calu3 W1282X cell lines when checked for the RNase1treated samples.(Figure 5.12 A, B) We thought to ourselves if these disome peaks observed are really any indication of collision on the mRNA, for this reason we subjected separately collected fractions from the profile to a capillary based blotting analysis Jess® for Znf598 which is a known marker as a collision sensing molecule in the cells. It is one of the primary makers which bind to the ubiquitination site of two collided ribosomes. Jess analysis revealed that Znf598 was highly elevated in the disome fraction of Calu3 W1282x cells line but not so much in the Calu3 WT cell line, indicating that the disome peak revealed is truly a collision peak only in the cell line which contains W1282X CFTR mRNA. We then checked if nonsense suppressor tRNA GEN3 has any effect on the disome peak and Znf598, when the cells were treated with GEN3 tRNA, the disome fraction subjected to Jess analysis had relatively reduced Znf598 expression indicating that suppressor tRNA addition dramatically reduced stable disome formation due to collisions in calu3 W1282X cell lines. (Figure 5.12 C)

We also know that stably collided ribosomes will activate downstream pathways, one of which is known to be the master regulator of downstream pathways when collision of ribosomes occurs, GCN1 has been known to be this master regulator. We then wanted to find out if there is even any fraction of possibly collided ribosomes that are bound by GCN1. We then probed the cell lysate fractions from calu3 WT and calu3 W1282X cell lines in JESS for GCN1, it co-precipitated to some degree along with all the fractions for calu3 WT and calu3 W1282X cells with RNase1 digestion and without. GCN1 was majorly localized in subunit and monosome fractions for calu3 WT cells indicating non bound state to collided ribosomes but for calu3 W1282X cells it was majorly localized in disome fraction which indicated stable collisions. (Figure 5.12 D)

All these collision indicators so far were detected on whole cell lysate of calu3 W1282X cells and not in calu3 WT cells, which indicates that collision could be a direct result of presence of PTC carrying CFTR mRNA in calu3 w1282X, but this was indirect evidence. To confirm our results and hypothesis that collision is a direct result of the PTC carrying CFTR mRNA, we subjected the same lysates to JESS for CFTR and Znf598 as a multiplex capillary electrophoresis. CFTR co-blotted with Znf598 in disome fraction for calu3 W1282X non-RNase digested sample, along with higher concentrations in polysome fraction, but it was not found to be co-blotted in calu3 WT cells in disome fraction but only CFTR was found in polysome fraction. (Figure 5.12

E(left)) This co-blotted CFTR and Znf598 in calu3 W1282X sample indicated that indeed the collisions originating were from W1282X CFTR mRNA. One thing to notice here was that the CFTR band in calu3 WT cells was a bit higher and we assume that the difference could be due truncated protein found in calu3 W1282X cells. Interestingly when the cells were supplemented with GEN3 tRNA, the co-blotted Znf596 with CFTR disappears and only CFTR band was seen in disome and polysome fraction. (Figure 5.12 E(right))

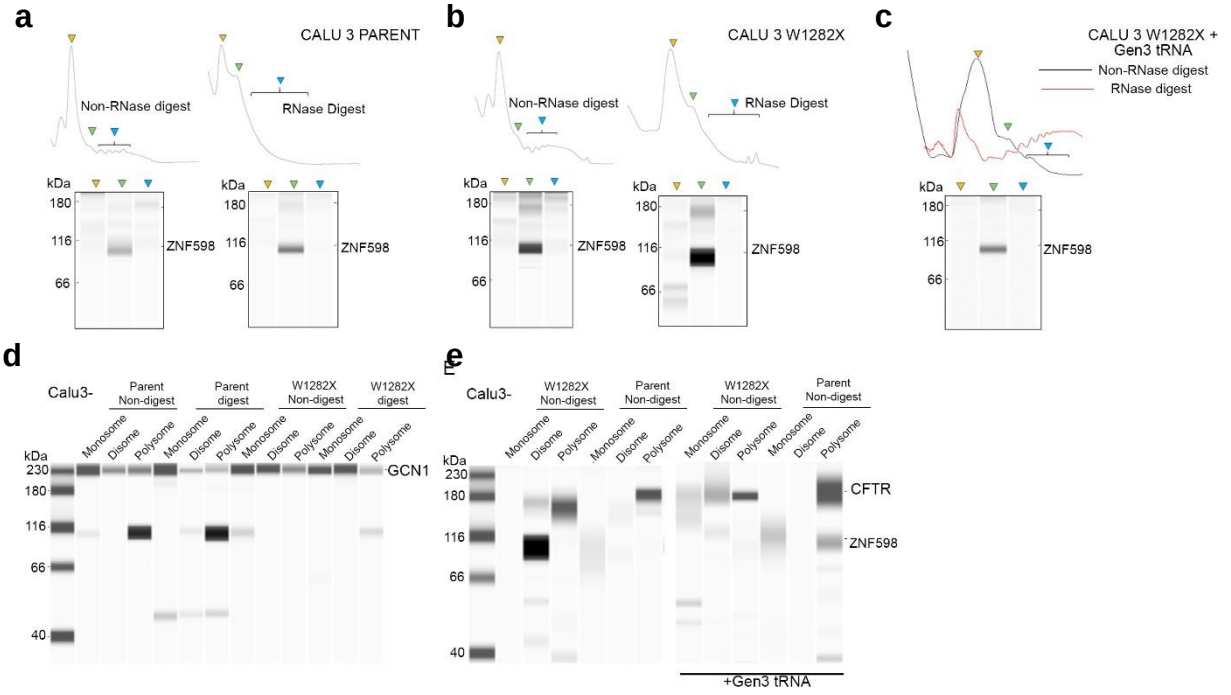

Figure 5.12 Collisions on W1282X PTC CFTR mRNA in callu3 cells A), B), C) are sucrose gradient profiles on sucrose gradient 15-60%, collected from calu3 W1282X and WT cells, which carry constitutively expressing CFTR mRNA with W1282X PTC and WT respectively, gradients were separated and collected into fractions representing different translational occupancy of ribosomes in the cell, monosome (yellow arrow), disome (green arrow) and polysome (blue arrow). Below for each is a capillary based western blot called JESS, where each fraction was immunoblotted for Znf598 Ab, which is a key marker for collisions. C) the jess blot shows lowered Znf598 found in disome fraction when treated with GEN3 suppressor tRNA compared to in B showing collision marker persistently present in disome fraction. D) GCN1 a key marker of persistent collision in cell activated in disome fractions of calu3 W1282X and not in calu3 WT. E) left co-blotting of znf598 and CFTR in W1282X disome fraction, showing that collisions are indeed on PTC and E) right showing that there is an absence of znf598 in W1282X disome fraction when treated with GEN3 suppressor tRNA, and CFTR band is highly present in polysome fraction, when compared to calu3 WT samples.

5.2.5 The collision effect is exacerbated when calu3 cells are treated with eukaryotic release factor-1 inhibitor.

Earlier results indicated that we could detect collisions in cell model system with a constitutively expressed W1282X CFTR mRNA. We were also able to observe co-blotting of collision marker Znf598 and CFTR in the disome fraction of cell lysates from calu3 W1282X cells, but we could see that collision were occurring only on a fraction of CFTR mRNA in the cell from the total lysates due to presence of a truncated protein CFTR band in polysome fraction. We wanted to see if we could simulate collisions where the number of ribosomes on the mRNA are limited. We then treated calu3 W1282X and WT cells with an eRF1 inhibitor SRI-41315, which blocks eRF1 from binding to the empty A-site of ribosome when it encounters a stop codon in the background of harringtonine treatment which inhibits translation initiation to have limited ribosomes on the mRNA, to capture better collided state of ribosome on W1282X CFTR mRNA. As it was expected, we co-blotted CFTR and Znf598 in disome fraction of calu3 W1282X cells, the Znf598 was also expressed at a higher level. (Figure 5.13 A) It was also observed that there was almost a non-existent CFTR band in polysome fraction of calu3 W1282X cells. Calu3 WT cells had similar results to earlier experiments, with no Znf598 expression in disome fraction but a full length highly glycosylated CFTR band in polysome fraction. With this exacerbated effect of eRF1 inhibitor, we wanted to check if these collisions provide a better opportunity for nonsense suppressor tRNA GEN3 to rescue the translation at PTC. We took the earlier used F.luc system with extended W1282X context along with W1282X extended Δ which would lower the sudden changes in speed as in figure 5.11 A, B transfected embedded in a plasmid vector in CFBE4o- cells. We treated the cells with eRF1 inhibitor and also a combination of eRF1 inhibitor with nonsense suppressor tRNA GEN3, we saw that rescue for W1282X extended Δ with eRF1 inhibitor and GEN3 suppressor tRNA (figure 5.13 B) was comparable to rescue we saw in short context readthrough with suppressor tRNA in figure 5.11 D, at the same time W1282X extended we could not see any change in rescue with treatment with eRF1 inhibitor and GEN3 suppressor. We suspect this was due to lowered collision probability on W1282X extended Δ allowed for single ribosome stuck at PTC stop codon with empty A site to be filled by nonsense suppressor tRNA GEN3 and allowed rapid rescue, but on the W1282X extended context there was a collision probability, due to sudden change in speed right before the PTC and collided ribosomes could only be rescued before the collision occurred which is why we observe low rescue of the same.

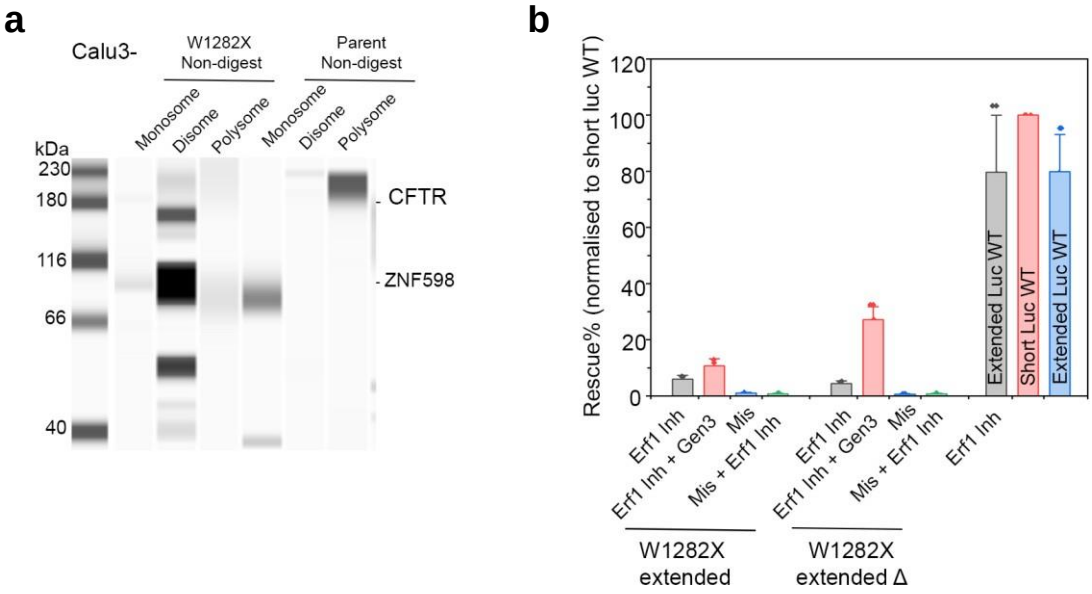

Figure 5.13: A) Jess immunoblot assay for calu3 W1282X and WT fractions by sucrose gradient 15-60% when they were treated with harringtonine (translation initiation inhibitor) and eRF1 inhibitor to mimic cellular collisions on W1282X PTC, it was observed that the effect in figure 5.12 E was highly exacerbated. B) Fluc based readthrough experiments on W1282X extended context and W1282X extended Δ context in eRF1 inhibitor background, showing no change in rescue with eRF1 inhibitor co treated with GEN3 tRNA for W1282X extended context but reached normal levels of rescue of a short context (figure 5.11 D) for W1282X extended Δ likely because the latter context is now speed optimized and collision probability is reduced

6 DISCUSSION

Our studies demonstrate that native tRNAs can be refactored to efficiently decode clinically important nonsense mutations. Repurposing of tRNAs to decode various nonsense mutation-derived PTCs, including the most difficult to correct UAA PTC, involves altering tRNA sequences that modulate decoding accuracy (118,120) (i.e., through AC-stem mutations) and binding affinity to elongation factor (119) (i.e. through modulation of the TΨC-stem), framed in terms of the individual thermodynamic contribution of the amino acid to be inserted at the PTC. At disease-causing PTCs, an optimized tRNA suppressor alone restored protein expression, function, and airway volume homeostasis in a manner relevant to CF clinical benefit – thus, in this case addition of NMD inhibitors as adjuvants may not be necessary. Although NMD inhibitors may lengthen the kinetic window for some drug-mediated readthrough strategies (136), dose and treatment to block NMD must be carefully tuned to avoid widespread mis regulation of gene expression (137).

With the establishment of nonsense suppressor tRNA having a therapeutic potential to suppress nonsense mutations in CFTR, we chose CFTR as a model system to address another important question of variability and accuracy of suppression. The results have shown that suppression of PTC did not have any suppression of natural termination codon above basal levels in WT CFTR. This accuracy and variability in rescue seen for arginine and serine PTC mutations were impending questions that needed to be resolved. These questions to some extent studied earlier when PTC suppression was aided using small molecules such as AAGs (128,135,138). PTC context is known to have an influence in its suppression when AAGs are used, this nature of sequence context influence may or may not have the same influence when using nonsense suppressor tRNAs. AAGs slow down termination events as ribosome encounters empty A site to allow near cognate tRNA to bind (128,139–141). Since we use suppressor tRNA to suppress PTC mutations, the order of timings that suppress PTC mutations change completely, for instance now the binding of suppressor tRNA would be similar to order of timings as any natural tRNA with its decoding rate. With this approach there are new challenges that come with using suppressor tRNA, it needs to outcompete termination factors such as eRF1 which have an order of binding as low as o.1seconds (142,143). These factors all together govern how accurately suppressor tRNA can suppress PTC mutations. Sequence context that have been earlier studied are based on AAG studies, we used the same context to study how much the sequence context influences suppressor tRNA efficacy on CFTR mutations (127,144–146). CFTR mutations served as a good model because CFTR have multiple stop codon mutations, those which serve as multiple possible sequence contexts on same mRNA body and reduce the number of variables. (https://cftr2.org/) We see that same suppressor tRNA GEN1, GEN2 and GEN3 had various

efficiency level when suppressing PTC mutations, in our preliminary results. W1282X UGA mutation was the one that could be rescued with highest efficiency of upwards of 65% when compared to mismatch tRNA and normalized by WT luciferase expression as shown in figure 5.7, with UAG mutations being suppressed the most and UAA mutations the least. With GEN3 tRNA being most efficient we decided to use GEN3 tRNA for all other experiments to reduce the number of variables. These results were only another validation of variability we see as shown in chapter1, tRNA based suppression is indeed governed by various factors.

We built an 'ideal' sequence which is a summation of all the sequence context studies that were done with AAGs for both 5' and 3' end sequences of PTC mutations with individual nucleotide effect, positions up to 9 nucleotides downstream and 6 nucleotides upstream (147). This ideal sequence allowed maximum suppression of PTC mutations as studied earlier. We compared upstream and downstream similarity of the ideal sequence with all CFTR PTC mutations and sorted them with their sequence similarity upstream and downstream as in figure 5.8. we further then selected mutations from each category were subjected to Fluc readthrough assay to measure dependence of sequence context on GEN3 tRNA, overall, we saw that there was a little more dependance on upstream sequence than the downstream sequence, especially for the highest rescued, W1282X. Dependance on upstream sequence in earlier studies was understood to be of less importance compared to upstream sequence context (148,149), this is one preliminary evidence we see that suppressor tRNA have different dependance on sequence context as understood earlier in case of AAGs. Moreover, the evidence is clearer that efficiency of suppressor tRNA is indeed dependent on multiple factors and is more than just a sequence context around the PTC mutation. We suspect there is a long way to characterize all the variables in play when suppressor tRNA recues a PTC mutation due to limitations in technology and knowledge of all the factors in play.

We also replicated rescue on full length CFTR mutations such as R1162X UGA in chapter 5.1 and the short context readthrough was able to predict how much rescue would occur shown in chapter 5.2. We hypothesized that upstream context may have more relevance when it comes to longer context than 7 codon sequence taken in Fluc reporter systems, we believed that ribosomes speed that is approaching the PTC may be a crucial factor how efficacy is regulated (150). To study this hypothesis, we designed extended sequence of up to 65 codons upstream for all CFTR mutations and via ribosome sequence data from CFBE4o- we were able to decipher codon speeds based on ribosome occupancy values. We generated speed profiles and interestingly we found out that W1282X UGA had sudden speed changes near the PTC, which caught our interest. We generated 35 codon Fluc reporter system of W1282X UGA including the region where sudden speed changes were occurring. W1282X extended. We also generated another similar reporter

system but with codons changed such that speed changes were not sudden anymore W1282X extended Δ. Rescue for both by GEN3 suppressor tRNA proved the hypothesis correct with W1282X extended context suppression was much reduced compared to short context Fluc reporter, which was corrected when W1282X extended Δ context was used. Providing valuable information on upstream ribosomes speed dependance on PTC rescue by nonsense suppressor tRNA. This is an unknown area when comes to rescuing PTC mutations, but as our work has shed light on the various factors that could be in play, it does make sense that speed or rate of translation around PTC mutations would affect suppressor tRNA binding to the A-site.

With sucrose gradient profiling of constitutively expressing full length W1282X CFTR mRNA in calu3 cells, we saw a persistent disome peak, a possible collision marker. Immunoblotting with Znf598 antibody a primary factor binding collisions (151) we were able to see that it is precipitated with the disome fraction in W1282X calu3 cells and not WT calu3 cells. This co precipitation of Znf598 was rescued by adding suppressor tRNA GEN3 to calu3 W1282X cells. We further confirmed that a percentage of these collisions were even very strong and not transient in nature with GCN1 a general quality stress response sensor (152,153) precipitating in disome fraction of calu3 W1282X cells. These results being on total cell lysate posed a question whether these collisions are indeed occurring on CFTR mRNA, with co-immunoblotting of Znf598 and CFTR for calu3 W1282X cells only when compared to calu3 WT cells. The direct evidence of collisions on W1282X CFTR mRNA showed that upstream context is much more important and maybe speed changes are responsible for such collision events which are not temporary. We mimicked cellular conditions where collisions would be evident and might inhibit translation initiation (154). We then by suppressing eRF1 (145) and inhibiting translation initiation in calu3 W1282X cells and we confirmed our hypothesis, collisions were even more exacerbated seen in calu3 W1282X cells by immunoblotting disome fractions of calu3 W1282X cells compared to calu3 WT cells. Further the ability of GEN3 suppressor tRNA to rescue W1282x extended Δ context compared to W1282X extended context in Fluc reporter system in background of erf1 inhibition, showed that PTC suppression is reduced when impeding collisions are probable due to upstream speed changes near PTC. These results shed light on possibility of ribosome collisions on PTC and how it may affect further work with suppressor tRNAs, this seems to be a new and a rather less know area when PTC rescue studies are concerned. We believe further work in the area would provide crucial information in paving way for treating diseases using suppressor tRNA in future

7 CONCLUSION

This study, therefore, provides a framework for development of tRNA-based PTC inhibitors administration that are shaped to an individual PTC context and relevant amino acid as a means to expression. precision and individualized therapy of hereditary diseases caused by nonsense mutations. We here provide a possible model where impending collisions due to speed changes upstream of a PTC mutation can lead to low suppression by nonsense suppressor tRNA in cells. This kind of information will provide us with a toolbox like information on PTC mutations correctability in future. Where based on our predictions using toolbox information, we would be able to fine tune suppressor tRNA efficacy needed for particular PTC suppression.

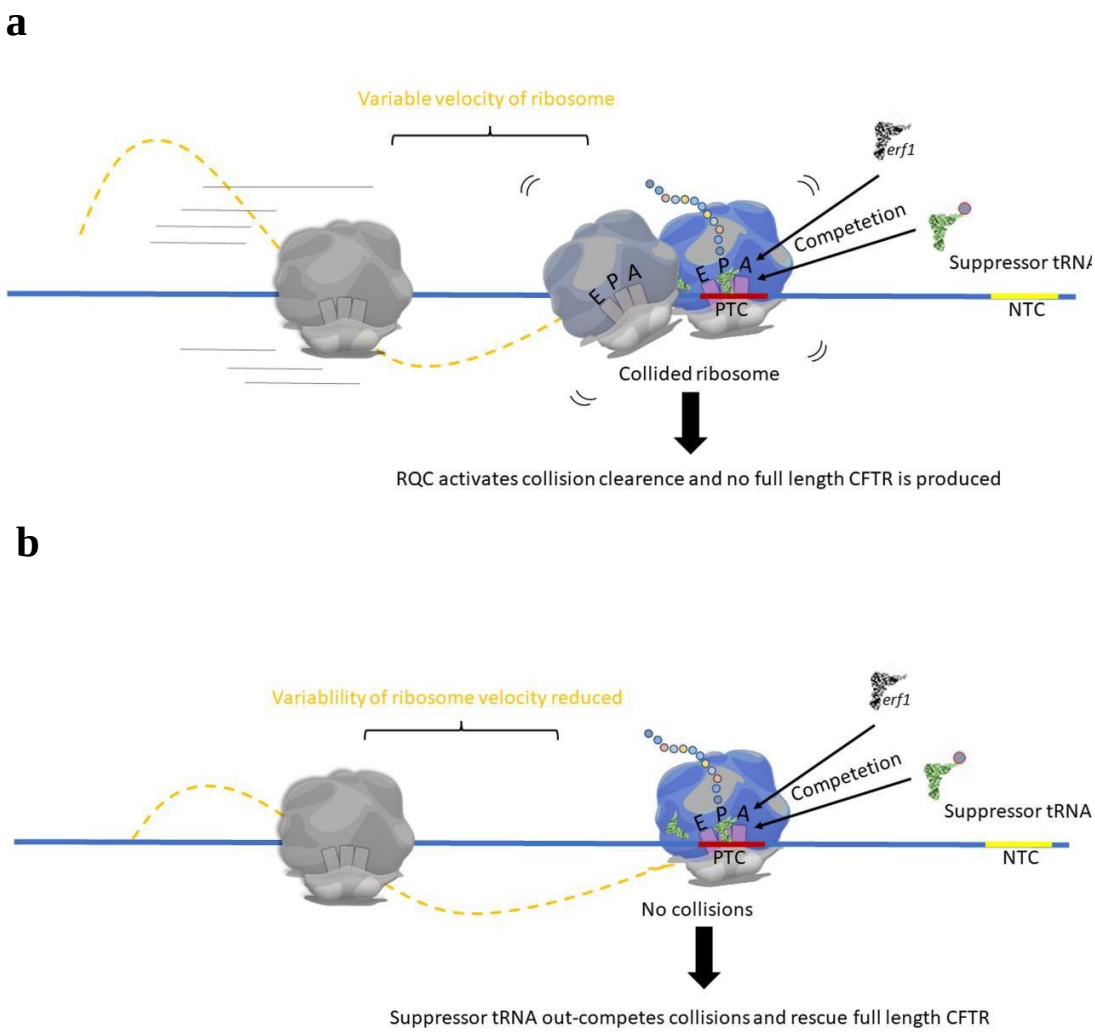

Figure 7.1 Model representing probable collision occurring on PTC mRNA where A) ribosome speed upstream the PTC has sudden changes which allows collision and lower suppression by nonsense suppressor tRNA, B) whereas when the variable speed is dampened the collision probability reduces allowing suppressor tRNA rescue PTC more efficiently.

8 Materials and Methods

Plasmid and RNA constructs

To test readthrough efficiency of suppressor tRNAs, we used two different constructs. (i) Dual Firefly luciferase-Renilla luciferase (FLuc-RLuc) reporter containing 15 codons from TPP1 (codons 201-215) downstream of the AUG codons of FLuc (FLuc-R208X-RLuc). As a control, when using the tSA1T5 suppressor charged with Ser, we replaced the UGA PTC in FLuc-R208X-RLuc with the AGC codon encoding Ser yielding FLuc-R208S-RLuc..

Cell lines and primary cells

Hep3B (HB-8064) and Hepa 1-6 (CRL-1830) cell lines were obtained from the ATCC. Cre-lox reporter was integrated in HEK293T (CRL-3216) cells (generated by Dr. Ramon Trelles, Arcturus Therapeutics). The immortalized CF bronchial epithelial cell line (Suppressor tRNA; generated by D. Gruenert, UCSF) with no allelic CFTR expression was used for ectopic expression of CFTR variants. Transepithelial ion transport was measured in Fischer rat thyroid (FRT) cells stably expressing R553X-CFTR or WT-CFTR.

Calu3 W1282X and Calu3 parental (WT) cell lines were obtained from Eric. J. Sorcher, at the Department of Pediatrics, Emory University School of Medicine, Atlanta, USA, Cells were transfected grown in DMEM with 10% FBS and no antibiotics. Cell lines were transfected with 200nf of suppressor tRNA for all the experiments. For Erf-1 inhibitor experiments, cells were treated with 5mM concentration of SRI-41315 from MedChem express.

16HBE14o- cells, the immortalized version of human bronchial epithelial cells expressing WT-CFTR (including all introns; generated by D. Gruenert, UCSF), were gene edited at the endogenous CFTR locus using CRISPR/Cas9 to create isogenic cell lines 16HBEge CFTR R553X/- and R1162X/- cell lines 37. 16HBEge cell lines were obtained from the Cystic Fibrosis Foundation Therapeutics Lab (Lexington MA, USA).

Primary human nasal epithelial (hNE) cells collected by nasal brush from a CF patient homozygous for R1162X/R1162X were we obtained them at passage 2 from the Cystic Fibrosis Foundation Therapeutics Lab (Lexington MA, USA).

tRNA design

In three isoacceptors, tRNASer(AGA) and tRNASer(UGA), tRNAArg(UCU) and tRNAGly(UCC), the anticodon was exchanged to produce the first generation tRNAs, tS, tR and tG, respectively Previous studies suggested that among the tRNA families, these isoacceptors, e.g. tRNASer(AGA) and tRNASer(UGA), tRNAArg(UCU) and tRNAGly(UCC)8 exhibited the highest readthrough following the exchange of their native anticodon to decode a stop codon.

For TΨC-stem tRNA variants, we estimated the ΔΔG° values for binding affinities to eEF1A considering the cumulative contribution of the three TΨC-stem base pairs, 49-65, 50-64 and 51-63 in each tRNA variant The ΔΔG° value for each nucleotide pair was taken from the bacterial EF-Tu-tRNAPhe complex20,38. Both AC stem and AC loop have coevolved with the anticodon to ensure faithful decoding. To increase the decoding, U-A or A-U pairs are preferred at nucleotide positions 31and 39 in native suppressor tRNAs39, thus, we considered them in our Ai variants. In the A2 variants, the AC stem is taken from tRNASec.

tRNA transcription and transfection

In vitro transcribed tRNA variants with intact CCA ends were used for co-transfection in the immortalized cell culture models, patient-derived primary cells

tRNAs were transcribed in vitro using T7 transcription system as described in13. Briefly, two partially overlapping DNA oligonucleotides encoding the corresponding tRNA sequence with an upstream T7 promoter (5'-TAATACGACTCACTATA-3') were used for in vitro tRNA synthesis. 24 µM of both oligonucleotides were denatured for 2 min at 95°C, thereafter aligned for 3 min at room temperature in 20 mM Tris-HCl (pH 7.5), 0.4 mM dNTPs were added and incubated with 4 U/µL RevertAid Reverse Transcriptase (Thermo Fisher Scientific) for 40 min at 37°C. This dsDNA template was purified with phenol/chloroform, washed with 80% EtOH and re-suspended in DEPC-H2O. For in vitro T7 transcription, 2 mM NTPs, 5 mM GMP, 1x transcription buffer, 0.6 U/µL T7 RNA polymerase (Thermo Fisher Scientific) were added to the dsDNA template and incubated overnight at 37°C. The tRNA variants were resolved by preparative denaturing polyacrylamide gel electrophoresis (PAGE) and eluted in 50 mM KOAc, 200 mM KCl pH 7.0 overnight at 4°C, followed by ethanol precipitation and re-suspension in DEPC-H2O.

Luciferase readthrough assay

Hep3B, Hepa 1-6 or Suppressor tRNA cells were seeded in 96-well cell culture plates at 1x104 cells/well and grown in Dulbecco´s Modified Essential Medium (DMEM, Pan Biotech) for Hep3B and Hepa 1-6 or Minimum Essential Medium (MEM, Pan Biotech) for Suppressor tRNA cells supplemented with 10% fetal bovine serum (FBS, Pan Biotech) and 2 mM L-glutamine (Thermo Fisher Scientific). 16 to 24 hours later, Hep3B or Suppressor tRNAcells were co-transfected in triplicate with 25 ng PTC-FLuc or WT-FLuc plasmids and 100 ng each in vitro transcribed tRNA variant using lipofectamine 3000 (Thermo Fisher Scientific). In an in vitro dose-response experiment 10-1000 ng of in vitro transcribed tRNA was co-transfected with the PTC-FLuc reporter plasmid (25 ng). After four to six hours, medium was replaced, and 24 hours post-transfection cells were lysed with 1x passive lysis buffer (Promega) and luciferase activity

measured with luciferase assay system (Promega) and Spark microplate reader (Tecan). G418 was added to the cells at concentration 25 µg/mL and incubated for 24 hours.

Hepa1-6 cells, 24 h after seeding, were transfected with 12.5 ng of one of the three in vitro transcribed reporter mRNAs (FLuc-R208X-RLuc; FLuc-R208S-RLuc or FLuc-R208-RLuc with Arg at position 208) together with 50 ng of in vitro transcribed tRNA using MessengerMax (0.2 µL/well). For in vitro dose-response experiment , 50-0.78 ng the in vitro transcribed tRNA was serially diluted by two-fold and co-transfected into each well with the reporter mRNA (12.5 ng). To achieve similar transfection efficiencies across different dosages of PTC-pairing tRNA, an in vitro transcribed mismatch tRNA that does not pair to the UGA PTC was used as filler so that total tRNA of 50 ng/well was always co-transfected. Cells were incubated at 37 °C overnight, rinsed with PBS and harvested by adding 20 µL/well of 1x passive lysis buffer (Promega). Luciferase activities were measured in 10 µL lysate with the Dual-Luciferase Reporter Assay kit (Promega) on Spark microplate reader (Tecan).

tRNA toxicity

CFBE 41o- cells were transfected with an in vitro transcribed suppressor tRNA in a concentration series from 1000-1.95 ng/well and serially diluted by two-fold as described above. Cell viability was determined using the CellTiter-Glo® luminescent cell viability assay (Promega) according to the manufacturer's instruction.

Stimulation of hTLR7/hTLR8 cells with tRNAs

IL-8 response in HEK293XL-hTLR7 or hTLR8 cells (Invivogen) was monitored as described in40. Briefly, HEK293XL stably transfected with hTLR7 and hTLR8 (Invivogen) were seeded in 96-well cell culture plates at 5x104 cells/well and cultured in DMEM supplemented with 10% FBS and 2 mM L-glutamine (Gibco). 24 hours later, cells were transfected with in vitro transcribed tSA2T5 (1 µg/mL) or resiquimod (R848; Invivogen, 1 µg/mL) as control activators of the TLR7/TLR8 signaling pathway41 using lipofectinTM (Thermo Fisher Scientific). After three hours, the medium was replaced and 16 hours post-transfections interleukin IL-8 in supernatants was measured using human IL-8 ELISA Kit II (BD Biosciences) according to the manufacturer's instructions.

Culturing of patient-derived nasal epithelial cells at the air-liquid interface (ALI)

2x106 hNE (R1162X/R1162X) cells were seeded in T75 flasks coated with collagen IV (Sigma) in 12 mL of pre-warmed complete Pneumacult Ex+ basal media (StemCell kit) supplemented with 3 mL hydrocortisone (StemCell), 2 mL of amphotericin B (12.5µg/mL; Sigma), 500µL ceftazidime (100mg/mL; Sigma), 500µL vancomycin (100mg/mL; Sigma), 500µL tobramycin

(100mg/mL; Sigma) and 10mL 50X Ex+ supplement (StemCell kit) at 37°C in 5% CO2 . Cells were expanded for approximately 5 days or until they reached 70-80% confluency.

Cells were then detached by 0,05% trypsin-EDTA treatment and seeded onto 12-well ALI plate (0.4 µm pore polyethylene terephtalate membrane inserts, Corning) coated with collagen 1V at a confluency of 1.5 x 105 – 2 x 105/well in 0.6 mL of Complete Ex+ media on the basolateral side and 0.1 mL on the apical side and grown at 37°C with 5% CO2. The Ex+ media contains 440 mL Pneumacult ALI basal medium, 50 mL of 10x ALI supplement, 5mL of 100x ALI maintenance supplement (StemCell), 2.5 mL of hydrocortisone (StemCell kit) and 1 mL heparin (StemCell kit). Cells were differentiated for 3 days with media changed every day on the apical and basolateral side. On day 4, the apical medium was removed and basolateral medium exchanged three times/week for at least 21 days until reaching a fully differentiated state. Primary patient-derived hNE cells are active in a short-time window post differentiation, i.e. 21-30 days and experiments ought to be performed in this widow. At later time points, although macroscopically unchanged, the transfection and expression efficiency largely decreases.

CFTR immunoblot expression analysis.

Suppressor tRNA cells or 16HBEge CFTR R1162X/- cells were seeded on 12-well cell culture plates at 1x105 cells/well and cultured in Minimum Essential Medium (MEM, Pan Biotech) supplemented with 10% FBS (Pan Biotech) and 2 mM L-glutamine (Thermo Fisher Scientific). The medium of 16HBEge cells was additionally supplemented with 1% penicillin/streptomycin (Gibco) and the culture plates were precoated with 1% human fibronectin (ThemoFischer Scientific), 1% bovine collagen type I (Advanced BioMatrix), 1% bovine serum albumin (Gibco). At 24 hours after seeding, Suppressor tRNA cells were co-transfected with 800 ng PTC-CFTR (S466X or R553X) or WT-CFTR plasmids and 400 ng in vitro transcribed tRNA variant using lipofectamine 3000 (Thermo Fisher Scientific). In the experiments with NMD inhibitor, 16HBEge cells were pre-treated with 5µM NMD14 for 24 hours and then transfected with 800ng of in-vitro transcribed tRNA variant using lipofectamine 3000 (Thermo Fisher Scientific). After four to six hours of tRNA transfection, medium was replaced and 24 hours post transfection cells were lysed with 80 µL of MNT buffer (10x; 300 mM Tris-HCl pH 7.5, 200 mM 2-(N-morpholino) ethanesulfonic acid (MES) and 1 M NaCl).

Fully differentiated hNE (R1162X/R1162X) cells (see above) were treated with 5 µM nonsense mediated decay inhibitor (NMD14; MedChemExpress) on the basolateral side. Six hours following addition of NMD inhibitor (5 µM NMD14 or 0.5 µM SMG1)35, 800-1000 ng in vitro transcribed tRNA (tRT5 or mismatch tRNA) was transfected from the apical surface of monolayers using lipofectamine 3000 (Thermo Fisher Scientific), while continuing treatment

with NMD14. After an additional 6 h (total treatment with NMD14 was 12 hours), fresh medium was exchanged and the cells incubated for the next 24h. Cells were then lysed with 80 µL of MNT buffer and lysate subjected to immunoblotting with monoclonal CFTR-NBD2 antibody (1:100 dilution, #596, John R. Riordan and Tim Jensen, University of North Carolina, Chapel Hill, USA) available through the Cystic Fibrosis Foundation Therapeutics Antibody Distribution Program (Bethesda, USA Company).Analysis utilized the capillary electrophoresis system (Jess, ProteinSimple) as described previously42. The peak area corresponding to fully glycosylated CFTR (band C) was normalized against total protein with the Jess quantification module. Band C intensity from samples transfected with suppressor tRNA +/- NMD inhibitor were normalized in comparison to intensity of band C from mock-transfected 16HBEge or hNE cells treated with NMD14, or from mismatch tRNA transfected Suppressor tRNA cells, respectively. Note that mock-transfected cells, i.e. treated with lipofectamine and water, should be used as a control due to the slight adverse effect of lipofectamine. Ataluren (PTC 124) was added at a final concentration of 10µM and 30µM and incubated for 24 hours.

Quantitative RT-PCR

The steady-state mRNA expression of CFTR variants transfected with in vitro transcribed tRNA variants (800 ng) or NMD inhibitor (5 µM) was measured using quantitative RT-PCR (qRT-PCR). Cells were grown as described above and treatedthe same way as described above for the immunoblot analysis, but to capture the expression on mRNA, cells were lysed after 6 hours of tRNA transfection (total 12h NMD14 and 6h of tRNA) . Total RNA was isolated using TriReagent (Sigma-Aldrich). 2 µg total RNA was reverse transcribed using random hexamers (Thermo Fisher Scientific) and RevertAid H Minus reverse transcriptase (Thermo Fischer) in 20 µl total volume. qPCR was performed using SensiMix SYBR® Hi-ROX Kit (Thermo Fisher Scientific) on T Professional thermocycler (Biometra). The region spanning exon 23-exon 24 (i.e. nucleotides 3874-4001 in the CFTR mRNA) of the CFTR transcript was amplified with the following primer pair: forward 5’-GATCGATGGTGTGTCTTGGGA-3’ and reverse 5’-TCCACTGTTCATAGGGATCCAA-3’. GusB transcript was used as a house-keeping expression control whose expression level ranges at the WT-CFTR expression and was amplified using the following primer pair: forward 5’-GACACGCTAGAGCATGAGGG-3’ and reverse 5’-GGGTGAGTGTGTTGTTGATGG-3’. The analysis was performed using ΔΔCT approach. Technical duplicates of each biological replicate reaction were carried out for each sample.

tRNA stability and tRNA-tailored microarrays

16HBEge CFTR R553X/- cells were seeded at 6x105 cells/well into precoated 6-well cell culture plates and grown as described above. 24 hours after seeding, cells were transfected with 1.5 µg

tSA2T5 or water (as control) in triplicates using lipofectamine 3000 according to the manufacturer´s protocol. Note that mock-transfected cells should be used as a control due to the slight adverse effect of lipofectamine. Cells were lysed at 5, 24, 36, 48 and 72 h post transfection, by adding 1 mL TRIzol/well (Invitrogen). Total RNA from cells was isolated using the TRIzol-method according to manufacturer's instructions and RNA integrity was assessed by 10%-denaturing polyacrylamide gel electrophoresis.

tRNAs were analyzed using tRNA-tailored microarrays as previously described43,44, with some adjustments to measure the suppressor tRNA. On the microarrays, tDNA probes covering the full-length tRNA sequence of the 41 cytoplasmic tRNA species complementary to 49 nuclear-encoding tRNA families are spotted, along with the tDNA (5´-TGGCGTAGTCGACGGGATTCGAACCCGTGCGGGGAAACCCCAACAGGTTTGAAGC CTGCCGCCTTAACCACTCGGCCACGACTAC-3´) complementary to tSA2T5. Each microarray consisted of 12 identical blocks, each containing 2 probes for each natural tRNA and tSA2T5 (i.e., in total 24 signals). To fully deacylate tRNAs, 5 µg of total RNA was incubated for 45 min at 37°C in 100 mM Tris-HCl buffer (pH 9.0), followed by purification by precipitation with ethanol and 0.1 volume of 3 M NaOAc (pH 5.5), supplemented with glycogen (20 mg/mL, Thermo Fisher Scientific). Cy3-labeled RNA:DNA hairpin oligonucleotide was ligated to deacylated 3'-NCCA ends of the tRNAs using T4 DNA ligase (NEB) for 1 h at room temperature. Total RNA from cells not transfected with tSA2T5 was used as comparison and labeled with Atto647-labeled RNA:DNA hairpin oligonucleotide. For subsequent normalization of the arrays, each sample was spiked in with three in vitro transcribed tRNAs (2 µM of each), which do not cross hybridize with any of the human tRNAs or the suppressor tRNA. Detailed experimental protocol for tRNA microarrays is available at protocols.io [doi:dx.doi.org/10.17504/protocols.io.hetb3en]. Scanned microarray slides were analyzed using inhouse Python scripts. The median of the ratio of Cy3/Atto647 signals was normalized to spike-ins whose ratio set to one. Thereafter, each single Cy3 signal from the suppressor tRNA was normalized to the Cy3 signal of the spike-ins and represented as a ratio to the mean of the signal at 5h which was set as 100%. The arrays were performed in two biological replicates for the samples withdrawn at 5, 24 and 36h post transfection, and in a single replicate for 48 and 72 h samples. Due to a high reproducibility of the arrays (confidence intervals higher than 98%), following the normalization to the spike-ins the individual signals from the biological duplicates were merged.

Short-circuit current Isc measurements.(done by collaobrators mentioned above)

Transepithelial ion transport was measured in FRT cells, which represent a standard model for polarizing epithelia expressing apical CFTR and are viewed by the US Food and Drug Administration as informative for drug label expansion for CFTR modulators45. FRT cells stably

expressing R553X-CFTR or WT-CFTR were seeded at 100,000-150,000 cells onto permeable supports (0.33 cm2 surface area inserts/transwells). Four days post seeding, cells form tight junctions and were transfected with in vitro transcribed 400 ng tRNA (tRT5 or mismatch tRNA) in 20 µL OptiMEM per insert using lipofectamine 3000 (Thermo Fisher Scientific). Cells were maintained under air-liquid interface conditions at 37°C in 5% CO2 for 24h. hNE (R1162X/R1162X) cells were cultured and transfected with 800 ng tRT5 or mismatch tRNA and treated with NMD inhibitor (0.5 µM SMG1)35 as described above before subjecting them to Isc measurements.

Short-circuit current was monitored under voltage clamp conditions with an MC8 voltage clamp and P2300 Ussing chamber equipment (Physiologic Instruments). Cells grown on culture inserts (Corning) were bathed on both sides with identical Ringer's solutions containing (in mM) 115 NaCl, 25 NaHCO3, 2.4 KH2PO4, 1.24 K2HPO4, 1.2 CaCl2, 1.2 MgCl2, and 10 D-glucose (pH 7.4). Solutions were aerated with 95% O2:5% CO2, and 1 second 3-mV pulses imposed every 10s to calculate resistance by Ohm's law. As indicated for the particular study, mucosal solutions were changed to a low chloride buffer (1.2 mM NaCl and 115 mM Na+ gluconate, with other components as above). Amiloride (100µM) was added (bilaterally) to block residual Na+ current, followed by the CFTR agonist forskolin (10µM) and CFTR potentiator VX770(5 µM). At the end of each experiment, Inh172 (10 µM, apically) was employed to block CFTR-dependent Isc. For analysis of Ussing chamber data, the ACQUIRE & ANALYZE 2.3 package (Physiologic Instruments) was run on windows environment software to measure current, voltage, conductance and resistance from 1 - 8 tissues simultaneously.

Functional assessment of airway surface by Micro-Optical Coherence Tomography (done by collaborators mentioned above)

For assessment of the functional microanatomic parameters (e.g. ASL volume) of hNE (R1162X/R1162X) transfected with tRT5 or mismatch tRNA, we used Micro-Optical Coherence Tomography (µOCT), a high-speed, high-resolution microscopic reflectance imaging approach, as described earlier46,47. Briefly, this is a non-invasive method, without using exogenous dyes and particles, to image airway epithelia and the associated quantitative analysis, and the µOCT instrument provides cross-sectional images of the cell monolayers at a resolution of approximately 1 µm. Images were acquired 1 mm from the filter periphery with a scanning beam parallel to the tangent of the circumference of the filter membrane disc. Data were acquired at 20,480 Hz line rate, resulting in 40 frames per second at 512 lines per frame. Quantification of the ASL volume was performed directly by geometric measurement of the corresponding layers in Image J software. Statistical analysis was performed by unpaired Student's t test or two-way ANOVA using Sidak's multiple comparisons.

Ribosome profiling and data analysis

20x106 Suppressor tRNA cells were co-transfected with 400 ng CFTR-R553X plasmid and 400 ng in vitro transcribed tRT6 or with 400 ng CFTR-WT plasmid alone using lipofectamine 3000 (Thermo Fisher Scientific). 24 hours post transfection, cells were harvested and lysed with lysis buffer (10 mM Tris-HCl pH 7.4, 5 mM MgCl2, 100 mM KCL, 1% NP-40, 2 mM DTT).

Lysates from Calu3 W1282X/WT or Suppressor tRNA cells were supplemented with cycloheximide (100 µg/ml) to prevent ribosomal dissociation during RNase I digestion (1.5 µL of 5U/OD260 for 30 min). For calu3 cells lysates after digestion were run on a sucrose gradient 15-60% at 35000rpm TW55ti rotor from Beckman Coulter® then were run on a gradient profiler at 254nm wavelength, then fractions were collected for each segment of profiles. These lysates were directly run on JESS machine as described earlier. Znf598 antibody was obtained from Abcam.

For Suppressor tRNA cells sequencing libraries from the RNase I digestion-derived ribosome-protected fragments (RPFs) were prepared using a protocol for miRNA with direct ligation of the adapters50.

Sequenced reads were quality selected using the fastx-toolkit (0.0.13.2) with a threshold of 20. Adapter sequences were removed by cutadap (1.8.3) with a minimal overlap of 1 nt. The libraries were depleted of reads mapping to rRNA reference sequences (bowtie 1.2.2; -y –un) and the reads were mapped to the human (GRCh38) and mouse (GRCm38) reference genomes, respectively. Mapping was performed using STAR51 (2.5.4b) allowing maximum of one mismatch and filtering out reads mapping to multiple positions (--outFilterMismatchNmax 1 --outFilterMultimapNmax 1). In the reference annotation files, the longest annotated CDS for each transcript was selected. For two transcripts of the same CDS length, we selected the longest transcript including 5’ and 3’UTRs. Uniquely mapped reads were normalized to reads per million mapped reads (RPM) or reads per kilobase per million mapped reads (RPKM).

To select transcripts that have undergone readthrough, we used the ribosome readthrough csore (RRTS) described in22. RRTS is a ratio of the mean read density over the CDS (RPK, i.e. normalized to the length) and the read density between the natural termination codon and next in-frame stop codon in the 3’UTRs (RPK, i.e. normalized to the length) separated by at least 3 nt from the natural stop codon of the CDSs. The CFTR transcript (ENSEMBL: ENSG00000001626; ENST00000003084.11) coverage is represented as RPM

9 References

1. Roux PP, Topisirovic I, Jackson RJ, Larsson O, Tian B, Sonenberg N, et al. Regulation of mRNA Translation by Signaling Pathways Regulation of mRNA Translation by Signaling Pathways. 2014;1–23.

2. Porse BT, Kirillov S V., Garrett RA. Antibiotics and the Peptidyltransferase Center. The Ribosome. 2014;441–9.

3. SCHERRER K, LATHAM H, DARNELL JE. Demonstration of an unstable RNA and of a precursor to ribosomal RNA in HeLa cells. Proc Natl Acad Sci U S A. 1963;49:240–8.

4. Baßler J, Hurt E. Eukaryotic Ribosome Assembly. Annu Rev Biochem. 2019;88:281–306.

5. Hershey JWB, Sonenberg N, Mathews MB. Principles of translational control: An overview. Cold Spring Harb Perspect Biol. 2012;4(12):1–10.

6. Dever TE, Dinman JD, Green R. Translation elongation and recoding in eukaryotes. Cold Spring Harb Perspect Biol. 2018;10(8):1–19.

7. Pestova T V., Borukhov SI, Hellen CUT. Eukaryotic ribosomes require initiation factors 1 and 1A to locate initiation codons. Nature. 1998;394(6696):854–9.

8. Rodnina M V., Wintermeyer W. Recent mechanistic insights into eukaryotic ribosomes. Curr Opin Cell Biol. 2009;21(3):435–43.

9. Pestova T V., Kolupaeva VG, Lomakin IB, Pilipenko E V., Shatsky IN, Agol VI, et al. Molecular mechanisms of translation initiation in eukaryotes. Proc Natl Acad Sci U S A. 2001;98(13):7029–36.

10. Morino S, Imataka H, Svitkin Y V., Pestova T V., Sonenberg N. Eukaryotic Translation Initiation Factor 4E (eIF4E) Binding Site and the Middle One-Third of eIF4GI Constitute the Core Domain for Cap-Dependent Translation, and the C-Terminal One-Third Functions as a Modulatory Region. Mol Cell Biol. 2000;20(2):468–77.

11. Passmore LA, Schmeing TM, Maag D, Applefield DJ, Acker MG, Algire MAA, et al. The Eukaryotic Translation Initiation Factors eIF1 and eIF1A Induce an Open Conformation of the 40S Ribosome. Mol Cell. 2007;26(1):41–50.

12. Aitken CE, Lorsch JR. A mechanistic overview of translation initiation in eukaryotes. Nat Struct Mol Biol. 2012;19(6):568–76.

13. Pestova T V., Lomakin IB, Lee JH, Choi SK, Dever TE, Hellen CUT. The joining of ribosomal subunits in eukaryotes requires eIF5B. Nature. 2000;403(6767):332–5.

14. Ribosomal T, Transferase P, Beringer M, Rodnina M V. Review. 2007;311–21.

15. Ogle JM, Ramakrishnan V. S i t f. 2005;

16. Blanchet S, Rowe M, Von Der Haar T, Fabret C, Demais S, Howard MJ, et al. New insights into stop codon recognition by eRF1. Nucleic Acids Res. 2015;43(6):3298–308.

17. Stansfield I, Jones KM, Kushnirov V V, Dagkesamanskayal AR, Poznyakovski A, Paushkin S V, et al. interact to mediate translation termination in Saccharomyces cerevisiae. 1995;14(17):4365–73.

18. Zhouravleva G, Frolova L, Goff X Le, Guellec R Le, Inge-vechtomov S, Kisselev L, et al. Termination of translation in eukaryotes is governed by two interacting polypeptide chain release factors , eRF1 and eRF3 Xenopus SUP35C. 1995;14(16):4065–72.

19. Alkalaeva EZ, Pisarev A V, Frolova LY, Kisselev LL, Pestova T V. In Vitro Reconstitution of Eukaryotic Translation Reveals Cooperativity between Release Factors eRF1 and eRF3. 2006;1125–36.

20. Hellen CUT. Translation Termination and Ribosome Recycling in Eukaryotes. 2018;1–18.

21. Bertram G, Bell HA, Ritchie DW, Fullerton G, Stansfield I. Terminating eukaryote translation : Domain 1 of release factor eRF1 functions in stop codon recognition. 2000;1236–47.

22. Frolova LY, Tsivkovskii RY, Sivolobova GF, Oparina NY, Serpinsky OI, Blinov VM, et al. Mutations in the highly conserved GGQ motif of class I polypeptide release factors abolish ability of human eRF1 to trigger peptidyl-tRNA hydrolysis. Rna. 1999;5(8):1014–20.

23. Hoshino S ichi, Imai M, Kobayashi T, Uchida N, Katada T. The Eukaryotic Polypeptide Chain Releasing Factor (eRF3/GSPT) Carrying the Translation Termination Signal to the 3â€²-Poly(A) Tail of mRNA. Journal of Biological Chemistry. 1999;274(24):16677–80.

24. Kozlov G, Gehring K. Molecular Basis of eRF3 Recognition by the MLLE Domain of Poly (A) -Binding Protein. 2010;5(4):3–8.

25. Neu-yilik G, Raimondeau E, Eliseev B, Yeramala L, Amthor B, Deniaud A, et al. Dual function of UPF 3 B in early and late translation termination. 2017;36(20):2968–86.

26. Hoshino S ichi, Imai M, Mizutani M, Kikuchi Y, Hanaoka F, Ui M, et al. Molecular Cloning of a Novel Member of the Eukaryotic Polypeptide Chain-Releasing Factors (eRF). Journal of Biological Chemistry. 1998;273(35):22254–9.

27. Salhi S, Goff C Le, Viranaicken W, Diop D, Jean-jean O. Involvement of Human Release Factors eRF3a and eRF3b in Translation Termination and Regulation of the Termination Complex Formation. 2005;25(14):5801–11.

28. Song H, Mugnier P, Das AK, Webb HM, Evans DR, Tuite MF, et al. The Crystal Structure of Human Eukaryotic Release Factor eRF1 — Mechanism of Stop Codon Recognition and Peptidyl-tRNA Hydrolysis. 2000;100:311–21.

29. Chavatte L, Seit-nebi A, Dubovaya V, Favre A. The invariant uridine of stop codons contacts the conserved NIKSR loop of human eRF1 in the ribosome. 2002;21(19).

30. Kolosov P, Frolova L, Seit-nebi A, Dubovaya V, Kononenko A, Oparina N, et al. Invariant amino acids essential for decoding function of polypeptide release factor eRF1. 2005;33(19):6418–25.

31. Bulygin KN, Khairulina YS, Kolosov PM, Yaminova AGVEN, Graifer DM, Vorobjev YN, et al. Three distinct peptides from the N domain of translation termination factor eRF1 surround stop codon in the ribosome. 2010;1902–14.

32. Brown A, Shao S, Murray J, Hegde RS, Ramakrishnan V. Structural basis for stop codon recognition in eukaryotes. Nature. 2015;524(7566):493–6.

33. Mccaughan KK, Brown CM, Dalphin ME, Berry MJ, Tate WP. Translational termination efficiency in mammals is influenced by the base following the stop codon. Proc Natl Acad Sci U S A. 1995;92(12):5431–5.

34. Shao S, Murray J, Brown A, Taunton J, Ramakrishnan V, Hegde RS. Decoding Mammalian Ribosome-mRNA States by Translational GTPase Complexes. Cell. 2016;167(5):1229-1240.e15.

35. Tate WP, Cridge AG, Brown CM. ‘Stop’ in protein synthesis is modulated with exquisite subtlety by an extended RNA translation signal. Biochem Soc Trans. 2018 Nov 12;46(6):1615–25.

36. Cheng Z, Saito K, Pisarev A V., Wada M, Pisareva VP, Pestova T V., et al. Structural insights into eRF3 and stop codon recognition by eRF1. Genes Dev. 2009;23(9):1106–18.

37. Conard SE, Buckley J, Dang M, Bedwell GJ, Carter RL, Khass M, et al. Identification of eRF1 residues that play critical and complementary roles in stop codon recognition. Rna. 2012;18(6):1210–21.

38. Shoemaker CJ, Green R. Kinetic analysis reveals the ordered coupling of translation termination and ribosome recycling in yeast. Proc Natl Acad Sci U S A. 2011;108(51).

39. Eyler DE, Wehner KA, Green R. Eukaryotic release factor 3 is required for multiple turnovers of peptide release catalysis by eukaryotic release factor 1. Journal of Biological Chemistry. 2013;288(41):29530–8.

40. Lawson MR, Lessen LN, Wang J, Prabhakar A, Corsepius NC, Green R, et al. Mechanisms that ensure speed and fidelity in eukaryotic translation termination. Science (1979). 2021;373(6557):876–82.

41. Keeling KM, Xue X, Gunn G, Bedwell DM. Therapeutics Based on Stop Codon Readthrough. 2014;

42. Wu CC chien, Zinshteyn B, Wehner KA, Green R. High-resolution ribosome profiling defines discrete ribosome elongation states and translational regulation during cellular stress. Mol Cell. 2019;73(5):959–70.

43. Shah P, Ding Y, Niemczyk M, Kudla G, Plotkin JB. Theory Rate-Limiting Steps in Yeast Protein Translation. Cell. 2013;153(7):1589–601.

44. Jacobson A. Upf1p , Nmd2p , and Upf3p Regulate the Decapping and Exonucleolytic Degradation of both Nonsense-Containing mRNAs and Wild-Type mRNAs. 2001;21(5):1515–30.

45. Potapova NA. Nonsense Mutations in Eukaryotes. 2022;87(5):400–12.

46. Gorlov IP, Kimmel M, Amos CI. Strength of the purifying selection against different categories of the point mutations in the coding regions of the human genome. Hum Mol Genet. 2006;15(7):1143–50.

47. Mort M, Ivanov D, Cooper DN, Chuzhanova NA. A meta-analysis of nonsense mutations causing human genetic disease. Hum Mutat. 2008;29(8):1037–47.

48. Hernandez-Gonzalez I, Tenorio-Castano J, Ochoa-Parra N, Gallego N, Pérez-Olivares C, Lago-Docampo M, et al. Novel genetic and molecular pathways in pulmonary arterial hypertension associated with connective tissue disease. Cells. 2021;10(6):1–10.

49. Guerreiro R, Brás J, Wojtas A, Rademakers R, Hardy J, Graff-Radford N. A nonsense mutation in PRNP associated with clinical Alzheimer's disease. Neurobiol Aging. 2014;35(11):2656.e13-2656.e16.

50. Nakamura K, Sekijima Y, Nagamatsu K, Yoshida K, Ikeda SI. A novel nonsense mutation in the TITF-1 gene in a Japanese family with benign hereditary chorea. J Neurol Sci. 2012;313(1–2):189–92.

51. Saint-Criq V, Gray MA. Role of CFTR in epithelial physiology. Cellular and Molecular Life Sciences. 2017;74(1):93–115.

52. Rowe SM, Verkman AS. Cystic fibrosis transmembrane regulator correctors and potentiators. Cold Spring Harb Perspect Biol. 2013;5(8).

53. Jordan IK, Kota KC, Cui G, Thompson CH, McCarty NA. Evolutionary and functional divergence between the cystic fibrosis transmembrane conductance regulator and related ATP-binding cassette transporters. Proc Natl Acad Sci U S A. 2008;105(48):18865–70.

54. Gadsby DC, Nairn AC. Regulation of CFTR channel gating. Trends Biochem Sci. 1994;19(11):513–8.

55. Ferec C, Cutting GR. Assessing the disease-liability of mutations in CFTR. Cold Spring Harb Perspect Med. 2012;2(12):1–13.

56. Pranke I, Bidou L, Martin N, Blanchet S, Hatton A, Karri S, et al. Factors influencing readthrough therapy for frequent cystic fibrosis premature termination codons. ERJ Open Res. 2018 Jan 1;4(1):80–2017.

57. Wilschanski M. Class 1 CF mutations. Front Pharmacol. 2012;3 JUN(June):1–3.

58. Tarpey PS, Lucy Raymond F, Nguyen LS, Rodriguez J, Hackett A, Vandeleur L, et al. Mutations in UPF3B, a member of the nonsense-mediated mRNA decay complex, cause syndromic and nonsyndromic mental retardation. Nat Genet. 2007;39(9):1127–33.

59. Huang L, Lou CH, Chan W, Shum EY, Shao A, Stone E, et al. RNA Homeostasis Governed by Cell Type-Specific and Branched Feedback Loops Acting on NMD. Mol Cell. 2011;43(6):950–61.

60. Chan WK, Huang L, Gudikote JP, Chang YF, Imam JS, MacLean JA, et al. An alternative branch of the nonsense-mediated decay pathway. EMBO Journal. 2007;26(7):1820–30.

61. Mendell JT, Sharifi NA, Meyers JL, Martinez-Murillo F, Dietz HC. Nonsense surveillance regulates expression of diverse classes of mammalian transcripts and mutes genomic noise. Nat Genet. 2004;36(10):1073–8.

62. A faux 3’-UTR promotes aberrant termination and tr...[Nature. 2004] - PubMed Result.

63. Ivanov P V., Gehring NH, Kunz JB, Hentze MW, Kulozik AE. Interactions between UPF1, eRFs, PABP and the exon junction complex suggest an integrated model for mammalian NMD pathways. EMBO Journal. 2008;27(5):736–47.

64. Behm-Ansmant I, Gatfield D, Rehwinkel J, Hilgers V, Izaurralde E. A conserved role for cytoplasmic poly(A)-binding protein 1 (PABPC1) in nonsense-mediated mRNA decay. EMBO Journal. 2007;26(6):1591–601.

65. Nicholson P, Yepiskoposyan H, Metze S, Orozco RZ, Kleinschmidt N, Mühlemann O, et al. Nonsense-mediated mRNA decay in human cells: Mechanistic insights, functions beyond quality control and the double-life of NMD factors. Cellular and Molecular Life Sciences. 2010;67(5):677–700.

66. Downloaded from rnajournal.cshlp.org on February 12, 2023 - Published by Cold Spring Harbor Laboratory Press.

67. Bhattacharya A, Czaplinski K, Trifillis P, He F, Jacobson A, Peltz SW. Characterization of the biochemical properties of the human Upf1 gene product that is involved in nonsense-mediated mRNA decay. 2000;1226–35.

68. Karousis ED, Gurzeler L adrian, Mühlemann O. Human NMD ensues independentaly of ribosome stalling. Nat Commun. (2020):1–12.

69. Kadlec J, Izaurralde E, Cusack S. The structural basis for the interaction between nonsense- mediated mRNA decay factors UPF2 and UPF3. 2004;11(4):330–7.

70. Chakrabarti S, Jayachandran U, Bonneau F, Fiorini F, Basquin C, Domcke S, et al. Article Molecular Mechanisms for the RNA-Dependent ATPase Activity of Upf1 and Its Regulation by Upf2. 2011;693–703.

71. Ramani AK, Nelson AC, Kapranov P, Bell I, Gingeras TR, Fraser AG. Open Access High resolution transcriptome maps for wild-type and nonsense-mediated decay-defective Caenorhabditis elegans. 2009;10(9).

72. Steiner S, Mohn F, Paillusson A, Mu O. EJC-independent degradation of nonsense immunoglobulin- m mRNA depends on 3 ¢ UTR length. 2006;13(5):2005–7.

73. Matsuda D, Hosoda N, Kim YK, Maquat LE. Failsafe nonsense-mediated mRNA decay does not detectably target eIF4E-bound mRNA. 2007;14(10):974–9.

74. Longman D, Plasterk RHA, Johnstone IL, Cáceres JF. Mechanistic insights and identification of two novel factors in the C . elegans NMD pathway. 2007;1075–85.

75. Singh G, Rebbapragada I, Lykke-andersen J. A Competition between Stimulators and Antagonists of Upf Complex Recruitment Governs Human Nonsense-Mediated mRNA Decay. 2008;6(4).

76. MacDonald CC, Grozdanov PN. Nonsense in the testis: multiple roles for nonsense-mediated decay revealed in male reproduction. Biol Reprod. 2017 May 1;96(5):939–47.

77. Rodnina M V, Korniy N, Klimova M, Karki P, Peng B zen, Senyushkina T, et al. Translational recoding : canonical translation mechanisms reinterpreted. 2020;48(3):1056–67.

78. Hashem Y, Unbehaun A, Grassucci RA, Taylor D, Hellen CUT, Pestova T V, et al. Structure of the mammalian ribosomal pre-termination complex associated with eRF1 eRF3 GDPNP. 2014;42(5):3409–18.

79. Processes B, High R. Biosynthetic Processes Requiring High Specificity. 1974;71(10):4135–9.

80. Ruusala T, Ehrenberg M, Kurland CG. Is there proofreading during polypeptide synthesis ? 1982;1(6):741–5.

81. Paddon C, Loayza D, Vangelista L, Solari R, Michaelis S. Analysis of the localization of STE6 / CFTR chimeras in a Saccharomyces cerevisiae model for the cystic fibrosis defect CFTR D F508. 1996;19:1007–17.

82. Limited IRLP. Nucleic Acids Research. 1985;13(17):6265–72.

83. Keeling KM, Bedwell DM. Suppression of nonsense mutations as a therapeutic approach to treat genetic diseases. 2011;(December):837–52.

84. Pfister P, Hobbie S, Vicens Q, Bˆttger EC, Westhof E. The Molecular Basis for A-Site Mutations Con- ferring Aminoglycoside Resistance : Relationship between Ribosomal Susceptibility and X-ray Crystal Structures. 2003;0215:1078–88.

85. Antibiotics A, Eustice DC, Wilhelm JM. Fidelity of the Eukaryotic Codon-Anticodon Interaction : Interference by. 1984;1462–7.

86. Tulkens PM. Aminoglycosides : Nephrotoxicity. 1999;43(5):1003–12.

87. Huth ME, Ricci AJ, Cheng AG. Mechanisms of Aminoglycoside Ototoxicity and Targets of Hair Cell Protection. 2011;2011.

88. Ebrahimi-fakhari D, Dillmann U, Flotats-bastardas M, Poryo M, Abdul-khaliq H, Shamdeen MG, et al. Off-Label Use of Ataluren in Four Non-ambulatory Patients With Duchenne Muscular Dystrophy : Effects on Cardiac and Pulmonary Function and Muscle Strength. 2018;6(October):1–5.

89. Kerem E. Pharmacologic therapy for stop mutations : how much CFTR activity is enough ? :547–52.

90. Robbrecht E, Manen JF, Schaack S, Gilbert C, Feschotte C, Moisy C, et al. Prevention of muscular dystrophy in mice by CRISPR/Cas9 – mediated editing of germline DNA. 2014;345(6201):1184–8.

91. Linde L, Boelz S, Nissim-rafinia M, Oren YS, Wilschanski M, Yaacov Y, et al. Nonsense-mediated mRNA decay affects nonsense transcript levels and governs response of cystic fibrosis patients to gentamicin. 2007;117(3):683–92.

92. Zhang F. CRISPR / Cas9 : Prospects and Challenges. 2015;26(7):409–10.

93. Alam F, Kamal MA, Gan SH, Wong KK, Sasongko TH. Therapeutic Suppression of Nonsense Mutation: An Emerging Target in Multiple Diseases and Thrombotic Disorders. 2017;1598–609.

94. Hagemeijer MC, Siegwart DJ, Strug LJ, Cebotaru L, Torres MJ, Sofoluwe A, et al. Translational research to enable personalized treatment of cystic fi brosis. Journal of Cystic Fibrosis. 2018;17(2):S46–51.

95. Bordeira-carric R, Ferreira D, Mateus DD, Pinheiro H, Pe AP, Santos MAS, et al. Rescue of wild-type E-cadherin expression from nonsense-mutated cancer cells by a suppressor-tRNA. 2014;(November 2013):1085–92.

96. Lueck JD, Yoon JS, Perales-puchalt A, Mackey AL, In DT, Behlke MA, et al. Engineered transfer RNAs for suppression of premature termination codons. (2019):1–11.

97. Albers S, Beckert B, Matthies MC, Mandava CS, Schuster R, Seuring C, et al. Repurposing tRNAs for nonsense suppression. Nat Commun. (2021):1–10.

98. Rodnina M V, Korniy N, Klimova M, Karki P, Peng B zen, Senyushkina T, et al. Translational recoding : canonical translation mechanisms reinterpreted. 2020;48(3):1056–67.

99. Keeling KM, Wang D, Conard SE, Bedwell DM, Keeling KM, Wang D, et al. Suppression of premature termination codons as a therapeutic approach uppression of premature termination codons as a. 2012;9238.

100. Bonetti B, Fu L, Moon J, Bedwell DM. Saccharomyces cerevisiae. 1995;334–45.

101. Chen C ying A, Shyu A bin. Mechanisms of deadenylation- dependent decay. 2011;(April):167–83.

102. Cosson B, Couturier A, Chabelskaya S, Kiktev D, Inge-vechtomov S, Philippe M, et al. Poly (A) -Binding Protein Acts in Translation Termination via Eukaryotic Release Factor 3 Interaction and Does Not Influence [PSI ♂] Propagation. 2002;22(10):3301–15.

103. Blanchet S, Cornu D, Argentini M, Namy O. New insights into the incorporation of natural suppressor tRNAs at stop codons in Saccharomyces cerevisiae. 2014;1–12.

104. Roy B, Leszyk JD, Mangus DA, Jacobson A. Nonsense suppression by near-cognate tRNAs employs alternative base pairing at codon positions 1 and 3. 2015;112(10).

105. Demeshkina N, Jenner L, Westhof E, Yusupov M, Yusupova G. New structural insights into the decoding mechanism : Translation infidelity via a G Á U pair with Watson – Crick geometry. 2013;587:1848–57.

106. Westhof E, Yusupov M, Yusupova G. Recognition of Watson-Crick base pairs : constraints and limits due to geometric selection and tautomerism. 2014;11(April).

107. Huang L, Low A, Damle SS, Keenan MM, Kuntz S, Murray SF, et al. Antisense suppression of the nonsense mediated decay factor Upf3b as a potential treatment for diseases caused by nonsense mutations. 2018;1–16.

108. Poel E De, Spelier S, Suen SWF, Kruisselbrink E, Graeber SY. Functional Restoration of CFTR Nonsense Mutations in Intestinal Organoids. Journal of Cystic Fibrosis. 2022;21(2):246–53.

109. Hinzpeter A, Aissat A, Becdeli A De, Bieth E, Sondo E, Martin N, et al. Alternative Splicing of In-Frame Exon Associated with Premature Termination Codons : Implications for. 2012;

110. Bidou L, Hatin I, Perez N, Allamand V, Panthier J j, Rousset J p. Premature stop codons involved in muscular dystrophies show a broad spectrum of readthrough efficiencies in response to gentamicin treatment. 2004;619–27.

111. Wangen JR, Green R. Stop codon context influences genome-wide stimulation of termination codon readthrough by aminoglycosides. Elife. 2020;9:1–29.

112. Namy O, Hatin I, Rousset JP. Impact of the six nucleotides downstream of the stop codon on translation termination. EMBO Rep. 2001;2(9):787–93.

113. Cridge AG, Crowe-Mcauliffe C, Mathew SF, Tate WP. Eukaryotic translational termination efficiency is influenced by the 3′ nucleotides within the ribosomal mRNA channel. Nucleic Acids Res. 2018;46(4):1927–44.

114. Cridge AG, Crowe-mcauliffe C, Mathew SF, Tate WP. Eukaryotic translational termination efficiency is influenced by the 3 nucleotides within the ribosomal mRNA channel. 2018;46(4):1927–44.

115. MANUVAKHOVA M, KEELING KIM, BEDWELL DM. Aminoglycoside antibiotics mediate context-dependent suppression of termination codons in a mammalian translation system. RNA. 2000/07/01. 2000;6(7):1044–55.

116. Tork S, Hatin I, Rousset J pierre. The major 5 ¢ determinant in stop codon read-through involves two adjacent adenines. 2004;32(2).

117. Harrell L, Melcher U, Atkins JF. Predominance of six different hexanucleotide recoding signals 3 ′ of read-through stop codons. 2017;30(9):2011–7.

118. Nguyen HA, Sunita S, Dunham CM. Disruption of evolutionarily correlated tRNA elements impairs accurate decoding. Proc Natl Acad Sci U S A [Internet]. 2020/06/29. 2020 Jul 14;117(28):16333–8. Available from: https://pubmed.ncbi.nlm.nih.gov/32601241

119. Schrader JM, Chapman SJ, Uhlenbeck OC. Tuning the affinity of aminoacyl-tRNA to elongation factor Tu for optimal decoding. Proc Natl Acad Sci U S A [Internet]. 2011/03/14. 2011 Mar 29;108(13):5215–20. Available from: https://pubmed.ncbi.nlm.nih.gov/21402928

120. Yarus M, Cline S, Raftery L, Wier P, Bradley D. The translational efficiency of tRNA is a property of the anticodon arm. Journal of Biological Chemistry [Internet]. 1986;261(23):10496–505. Available from: http://dx.doi.org/10.1016/s0021-9258(18)67412-5

121. Ramaswamy S, Tonnu N, Tachikawa K, Limphong P, Vega JB, Karmali PP, et al. Systemic delivery of factor IX messenger RNA for protein replacement therapy. Proc Natl

Acad Sci U S A [Internet]. 2017/02/15. 2017 Mar 7;114(10):E1941–50. Available from: https://pubmed.ncbi.nlm.nih.gov/28202722

122. Mort M, Ivanov D, Cooper DN, Chuzhanova NA. A meta-analysis of nonsense mutations causing human genetic disease. Hum Mutat [Internet]. 2008;29(8):1037–47. Available from: http://dx.doi.org/10.1002/humu.20763

123. Grosjean H, Westhof E. An integrated, structure- and energy-based view of the genetic code. Nucleic Acids Res [Internet]. 2016/07/22. 2016 Sep 30;44(17):8020–40. Available from: https://pubmed.ncbi.nlm.nih.gov/27448410

124. Uhlenbeck OC, Schrader JM. Evolutionary tuning impacts the design of bacterial tRNAs for the incorporation of unnatural amino acids by ribosomes. Curr Opin Chem Biol [Internet]. 2018/07/27. 2018 Oct;46:138–45. Available from: https://pubmed.ncbi.nlm.nih.gov/30059836

125. Albers S, Beckert B, Matthies MC, Mandava CS, Schuster R, Seuring C, et al. Repurposing tRNAs for nonsense suppression. Nat Commun [Internet]. 2021 Jun 22;12(1):3850. Available from: https://pubmed.ncbi.nlm.nih.gov/34158503

126. Andersen GR, Pedersen L, Valente L, Chatterjee I, Kinzy TG, Kjeldgaard M, et al. Structural Basis for Nucleotide Exchange and Competition with tRNA in the Yeast Elongation Factor Complex eEF1A:eEF1Bα. Mol Cell [Internet]. 2000;6(5):1261–6. Available from: http://dx.doi.org/10.1016/s1097-2765(00)00122-2

127. McCague AF, Raraigh KS, Pellicore MJ, Davis-Marcisak EF, Evans TA, Han ST, et al. Correlating Cystic Fibrosis Transmembrane Conductance Regulator Function with Clinical Features to Inform Precision Treatment of Cystic Fibrosis. Am J Respir Crit Care Med [Internet]. 2019 May 1;199(9):1116–26. Available from: https://pubmed.ncbi.nlm.nih.gov/30888834

128. Wangen JR, Green R. Stop codon context influences genome-wide stimulation of termination codon readthrough by aminoglycosides. Elife. 2020;9:1–29.

129. Karousis ED, Mühlemann O. Nonsense-mediated mRNA decay begins where translation ends. Cold Spring Harb Perspect Biol. 2019;11(2):1–18.

130. Karousis ED, Gurzeler LA, Annibaldis G, Dreos R, Mühlemann O. Human NMD ensues independently of stable ribosome stalling. Nat Commun. 2020;11(1):4134.

131. McDonald CM, Campbell C, Torricelli RE, Finkel RS, Flanigan KM, Goemans N, et al. Ataluren in patients with nonsense mutation Duchenne muscular dystrophy (ACT DMD):

a multicentre, randomised, double-blind, placebo-controlled, phase 3 trial. The Lancet. 2017;390(10101):1489–98.

132. Roy B, Friesen WJ, Tomizawa Y, Leszyk JD, Zhuo J, Johnson B, et al. Ataluren stimulates ribosomal selection of near-cognate tRNAs to promote nonsense suppression. Proc Natl Acad Sci U S A. 2016;113(44):12508–13.

133. Supek F, Lehner B, Lindeboom RGH. To NMD or Not To NMD: Nonsense-mediated mRNA Decay in cancer and other genetic diseases. Trends in Genetics. 2021;37(7):657–68.

134. Mccaughan KK, Brown CM, Dalphin ME, Berry MJ, Tate WP. Translational termination efficiency in mammals is influenced by the base following the stop codon. Proc Natl Acad Sci U S A. 1995;92(12):5431–5.

135. Namy O, Hatin I, Rousset JP. Impact of the six nucleotides downstream of the stop codon on translation termination. EMBO Rep. 2001;2(9):787–93.

136. Floquet C, Hatin I, Rousset JP, Bidou L. Statistical analysis of readthrough levels for nonsense mutations in mammalian cells reveals a major determinant of response to gentamicin. PLoS Genet [Internet]. 2012/03/29. 2012;8(3):e1002608–e1002608. Available from: https://pubmed.ncbi.nlm.nih.gov/22479203

137. Supek F, Lehner B, Lindeboom RGH. To NMD or Not To NMD: Nonsense-Mediated mRNA Decay in Cancer and Other Genetic Diseases. Trends in Genetics [Internet]. 2021;37(7):657–68. Available from: http://dx.doi.org/10.1016/j.tig.2020.11.002

138. Conard SE, Buckley J, Dang M, Bedwell GJ, Carter RL, Khass M, et al. Identification of eRF1 residues that play critical and complementary roles in stop codon recognition. Rna. 2012;18(6):1210–21.

139. Cridge AG, Crowe-Mcauliffe C, Mathew SF, Tate WP. Eukaryotic translational termination efficiency is influenced by the 3′ nucleotides within the ribosomal mRNA channel. Nucleic Acids Res. 2018;46(4):1927–44.

140. Mccaughan KK, Brown CM, Dalphin ME, Berry MJ, Tate WP. Translational termination efficiency in mammals is influenced by the base following the stop codon. Proc Natl Acad Sci U S A. 1995;92(12):5431–5.

141. Shoemaker CJ, Green R. Kinetic analysis reveals the ordered coupling of translation termination and ribosome recycling in yeast. Proc Natl Acad Sci U S A. 2011;108(51).

142. Lawson MR, Lessen LN, Wang J, Prabhakar A, Corsepius NC, Green R, et al. Mechanisms that ensure speed and fidelity in eukaryotic translation termination. Science (1979). 2021;373(6557):876–82.

143. Song H, Mugnier P, Das AK, Webb HM, Evans DR, Tuite MF, et al. The Crystal Structure of Human Eukaryotic Release Factor eRF1 — Mechanism of Stop Codon Recognition and Peptidyl-tRNA Hydrolysis. 2000;100:311–21.

144. Ferec C, Cutting GR. Assessing the disease-liability of mutations in CFTR. Cold Spring Harb Perspect Med. 2012;2(12).

145. Sharma J, Du M, Wong E, Mutyam V, Li Y, Chen J, et al. A small molecule that induces translational readthrough of CFTR nonsense mutations by eRF1 depletion. Nat Commun. 2021 Dec 1;12(1).

146. Gambari R, Breveglieri G, Salvatori F, Alessia Finotti, Borgatti M. Therapy for Cystic Fibrosis Caused by Nonsense Mutations. In: Wat D, editor. Cystic Fibrosis in the Light of New Research [Internet]. Rijeka: IntechOpen; 2015. p. Ch. 13. Available from: https://doi.org/10.5772/61053

147. Namy O, Hatin I, Rousset JP. Impact of the six nucleotides downstream of the stop codon on translation termination. EMBO Rep. 2001;2(9):787–93.

148. Biziaev N, Sokolova E, Yanvarev D v., Toropygin IY, Shuvalov A, Egorova T, et al. Recognition of 3′ nucleotide context and stop codon readthrough are determined during mRNA translation elongation. Journal of Biological Chemistry. 2022 Jul 1;298(7).

149. Cridge AG, Crowe-Mcauliffe C, Mathew SF, Tate WP. Eukaryotic translational termination efficiency is influenced by the 3′ nucleotides within the ribosomal mRNA channel. Nucleic Acids Res. 2018 Feb 28;46(4):1927–44.

150. Li C, Zhang J. Stop-codon read-through arises largely from molecular errors and is generally nonadaptive. PLoS Genet. 2019 May 1;15(5).

151. Juszkiewicz S, Chandrasekaran V, Lin Z, Kraatz S, Ramakrishnan V, Hegde RS. ZNF598 Is a Quality Control Sensor of Collided Ribosomes. Mol Cell. 2018 Nov 1;72(3):469-481.e7.

152. Pochopien AA, Beckert B, Kasvandik S, Berninghausen O, Beckmann R, Tenson T, et al. Structure of Gcn1 bound to stalled and colliding 80S ribosomes. Available from: https://doi.org/10.1073/pnas.2022756118

153. Wu CCC, Peterson A, Zinshteyn B, Regot S, Green R. Ribosome Collisions Trigger General Stress Responses to Regulate Cell Fate. Cell. 2020 Jul 23;182(2):404-416.e14.

154. Juszkiewicz S, Slodkowicz G, Lin Z, Freire-Pritchett P, Peak-Chew SY, Hegde RS. Ribosome collisions trigger cis-acting feedback inhibition of translation initiation. Elife. 2020 Jul 1;9:1–29.

List of the hazardous substances used by GHS (hazard symbols, H&P statements)

Substance	Pictogram	Signal word	Hazard statements	Precautionary statements
2-[4-(2-hydroxy-ethyl)piperazin-1-yl] ethane-sulfonic acid (HEPES)	Not a dangerous substance according to GHS			
2-Mercaptoethanol		Danger	301+331, 310, 315, 317, 318, 373, 410	273, 280, 302+352, 304+340, 305+351+338, 308+310
Acetone		Danger	225, 319, 336	201, 305+351+338, 370+378, 403+235
Acrylamide/Bis-acrylamide		Danger	302+332, 315, 317, 319, 340, 350, 361f, 372	201, 261, 280, 304+340+312, 305+351+338, 308+313
Agaro	Not a dangerous substance according to GHS			
Ammonium acetate	Not a dangerous substance according to GHS			
Ammonium persulfate		Danger	272, 302, 315, 317, 319, 334, 335	220, 261, 280, 305+351+338, 342+311
Ampicillin		Danger	315, 317, 319, 334, 335	261, 280, 305+351+338, 342+311
Bromophenol blue	Not a dangerous substance according to GHS			

Chloramphenicol		Warning	351	280
Chloroform		Danger	302, 331, 315, 319, 351, 361d, 336, 372	261, 281, 305+351+3
Dimethyl sulfoxide	Not a dangerous substance according to GHS			201, 280, 301+330+331,
Dimethyl sulfate		Danger	330, 341, 350	302+352, 304+340, 305+351+338, 308+310
Dithiothreitol		Warning	302, 315, 319, 335	261, 305+351+338
Ethanol		Danger	225, 319	210, 240, 305+351+338, 403+233
Ethylenediamine-tetraacetic acid		Warning	319, 332, 373	280, 304+340, 312, 305+351+338, 337+313 261, 280
Folinic acid		Danger	334, 335	305+351+338, 342+311
Formamide		Danger	315, 360D, 373	201, 314
Glycerol	Not a dangerous substance according to GHS			
Glycin		Warning	315, 319, 335	261, 305+351+338

Hydrogen peroxide (30%)		Danger	302, 318	280, 305+351+338, 210, 233, 240,
Isopropyl alcohol		Danger	225, 319, 336	
LB-Agar	Not a dangerous substance according to GHS			
LB-Medium	Not a dangerous substance according to GHS			
Luminol	Not a dangerous substance according to GHS			
Magnesium acetate	Not a dangerous substance according to GHS			
Magnesium chloride	Not a dangerous substance according to GHS			
p-Coumaric acid		Warning	315, 319, 335	261, 305+351+338
PEG 8000	Not a dangerous substance according to GHS			
Phenol		Danger	301+311+331, 314, 341, 373, 411	260, 280, 301+330+331+310, 303+361+353, 304+340+310, 305+351+338
Phosphoenol-pyruvate	Not a dangerous substance according to GHS			
Potassium acetate	Not a dangerous substance according to GHS			
Potassium chloride	Not a dangerous substance according to GHS			
Potassium dihydrogen phosphate	Not a dangerous substance according to GHS			
RedSafe	Not a dangerous substance according to GHS			
Sodium acetate	Not a dangerous substance according to GHS			
Sodium azide		Danger	300+310, 373, 410	273, 280, 301+310+330, 302+352+310, 391, 501

Sodium chloride	Not a dangerous substance according to GHS			
Sodium dodecyl sulfate		Danger	228, 302+332, 315, 318, 335, 412	210, 261, 280, 301+312+330, 305+351+338+310, 370+378
Sodium hydrogen phosphate	Not a dangerous substance according to GHS			
SYBR Gold		Warning	227	210, 280, 370+378
Tetramethyl-ethylenediamine		Danger	225, 332, 302, 314	210, 280, 305+351+338, 310
Thiamine	Not a dangerous substance according to GHS			
TRIS acetate	Not a dangerous substance according to GHS			
Trisodium citrate	Not a dangerous substance according to GHS			201, 261, 264, 280, 273, 301+310,
TRIzol		Danger	314, 335, 341, 373, 412	302+352, 303+361+353, 304+340, 305+351+338

Tween 20	Not a dangerous substance according to GHS			
Urea	Not a dangerous substance according to			
Xylene cyanol FF		Warning	315, 319, 335	261, 305+351+338

10 Acknowledgements

With all my heart I would like to acknowledge all those who have helped me and guided me through all the decisions that have led me to pursue and finish my PhD.

First and foremost, I would like to thank Prof. Zoya Ignatova for giving me the opportunity and guidance throughout and for creating a free-thinking environment for me where I could grow my scientific knowledge and freely express my intent in the labs which has made me a better scientist. I also express my deep gratitude to Prof. Meliha Karsak, for the rich scientific discussion during the seminar and meetings. I also owe a deep gratitude to Dr. Suki Albers for her support and guidance since day1 of me joining labs, I thank her for also imparting great scientific knowledge all these years.

I owe a deep sense of gratitude to my parent, Mrs. Pooja Bharti and Mr. Chaman lal Bharti, and my sister Ms. Himani Bharti, who have been a constant support morally with kindness, enthusiasm and believing in me that have enabled me to complete my thesis.

There have been a lot of people because of which I was able to inculcate scientific integrity and knowledge my gratitude to all my previous supervisor and guides: Prof. Sankarganesh Arunachalam for seeding the knowledge of scientific process, Prof. Chetana Sachidanandan along with Dr. Sandeep Basu and Dr. Urmila Jagtap for their invaluable role in my life as a young scientist, it is only because of them I can uphold high principles of scientific integrity and I owe them for all the support and help I received for my time as a young scientist.

I would like to thank all my ex-startup partners Neelesh Agrawal, Dhiren Gupta and Utkarsh Ahluwalia for their support and sacrifice towards my decision to come to Hamburg and pursue my PhD.

Along with that I deeply thank my Lab members for the help and vivid discussions during seminar, coffee breaks and meeting. I specially thank Robin Thompson, Moritz Fryberg, Marcos Davyt and Dr.Sarada Das who have been amazing peers and great friends outside the lab, they have supported me through all the ups and downs of an expat living away from family and friends, I thank them for all the support and love. Along with this I also thank Dr. Klara Szydlo, Leonardo Santos, Negar and Christine Polte for their constant moral support.

And finally, to all the lab members for all their help with everyday tiny details that go unnoticed but one’s PhD is impossible without having such great peers in the Lab with scientific and friendly cheers.

11.EIDESSTATTLICHE VERSICHERUNG

Hiermit erkläre ich an Eides statt, die vorliegende Dissertation selbst verfasst und keine ande-ren als die angegebenen Hilfsmittel benutzt zu haben sowie diese Arbeit nicht zuvor an anderer Stelle eingereicht zu haben.

8.11.2023
Hamburg, den

Nikhil Bharti

Document identifier urn:nbn:de:gbv:18-ediss-113137